Dresden Unit 3
Core Spray Flaw Evaluation Report
Sargent & Lundy Project No. 10128-051
SL-5130, Rev. 2

June 3, 1997

Prepared By: Robert Geier / T.J. Behringer
Robert Geier, Engineer

T. Martel
T. Martel , Component Engineer

S. Lange
S. Lange, Piping System Engineer

Reviewed By: A. Al-Dabbagh / S. Singh
Dr. A. Al-Dabbagh, SE- Project Engineer

C. M. Launi
C. M. Launi, - PE, Senior Project Engineer

Approved By: Thomas J. Behringer
Thomas J. Behringer, PE, SE - Project Manager

ComEd Acceptance Review By: Guy D. DeBoo
Guy DeBoo, PE - Senior Staff Engineer

SARGENT & LUNDY CERTIFICATION OF REPORT NO. SL-5130

REV. 2

Dresden Unit 3
Core Spray Flaw Evaluation Report

I certify that this Design Document was prepared by me or under my supervision and that I am a Registered Engineer under the laws of the State of Illinois.

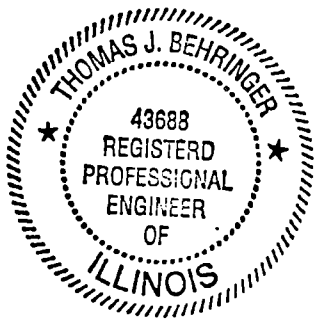

Thomas J. Behringer 6/3/97

Thomas J. Behringer
Project Manager

Dresden Unit 3
Core Spray Flaw Evaluation Report

DESIGN REPORT TABLE OF CONTENTS

LIST OF TABLES

LIST OF FIGURES

1.0 EXECUTIVE SUMMARY

During D3R14, inspections were performed of the reactor internal core spray system consisting of an ultrasonic examination of the piping welds from the reactor vessel nozzles down to the shroud and visual examinations of the sparger piping inside the shroud. All supports and brackets inside and outside the shroud were visually examined. Indications were observed at five locations on the Core Spray downcomers in the vessel annulus.

This flaw evaluation report provides a summary of the evaluation criteria, design inputs and the result of the evaluations performed to assess the extent, causes and impact of the cracking on the safe operation of the plant. The indications are typical of IGSCC in stainless steel. To demonstrate structural integrity, these indications were treated as IGSCC flaws and evaluated using ASME Section XI Appendix C flaw evaluation methods with the industry bounding IGSCC growth rate of $5x10^{-5}$ inches per hour. ComEd has evaluated the maximum impact of the leakage from these flaws on peak cladding temperature (PCT) during the DBA-LOCA in combination with the bounding single failure. This evaluation demonstrated that the peak cladding temperature during the DBA-LOCA would remain below 2200°F. In addition, beyond-design-basis bounding assessments using both the probabilistic and deterministic approach were made. These bounding assessments found that even with an assumed full circumferential failure of any one of the four downcomers, adequate core cooling would be maintained under all design basis events. The worst case scenarios (reactor recirculation suction line failure combined with a LPCI failure or a reactor recirculation failure combined with a LPCI failure and an SSE) present an insignificant risk since their probabilities are less than $1x10^{-06}$/year. Failure of a Core Spray downcomer could potentially result in a loose part and debris within the vessel. ComEd has evaluated the impact of loose parts and debris, and since the large pieces would be confined to the annulus region, no safety concerns were identified. ComEd will continue to monitor the condition of the degraded core spray welds per the recommendations provided in BWRVIP-18, BWR Core Spray Internals Inspection and Flaw Evaluation Guidelines, during subsequent refueling outages.

2.0 INTRODUCTION

The portion of the core spray line addressed in this condition assessment is located in the reactor pressure vessel (RPV) annulus of Dresden Unit 3. The RPV annulus portion of the core spray piping lines consists of two symmetrical loops with RPV penetrations at the 5° and 185° azimuths. These two loops feed the upper (80° and 290° downcomers; loop A) and lower (110° and 260° downcomers; Loop B) core spray spargers through shroud penetrations. A typical representation of this section of piping is illustrated with weld designations in Figure 2.1.

In April of 1997, Dresden Plant Engineering initiated the planned D3R14 examinations of the internal core spray piping. The inspection scope consisted of automated ultrasonic examination of all core spray piping welds from the junction box at the RPV nozzle to the downcomer connection at the shroud. Where access restrictions prevented 100% ultrasonic coverage of a given weld, supplemental enhanced visual examination (EVT-1) was performed to ensure 100% coverage of the weld, where possible. Additionally, enhanced visual examination was also performed on the elbow to shroud pipe welds (P4D) and the shroud pipe to collar welds (P8A), because the ultrasonic techniques employed at these locations have not yet been fully qualified per BWRVIP-03, Reactor Pressure Vessel and Internals Examination Guidelines. However, it should be noted that 100% ultrasonic coverage was achieved at these locations and that the examinations were able to detect and size the indications recorded in the P8A welds.

Internal to the shroud, enhanced visual examinations were performed on the core spray sparger tee-box cover plate welds, sparger to tee-box branch connection welds and sparger end cap welds. Also, modified VT-1 (MVT-1) examinations were performed on the sparger nozzles, piping, brackets and gusset welds (Reference 4).

The internal core spray visual examinations conducted during the previous Unit 3 refuel outage (D3R13) identified flaws in the downcomer pipe to lower elbow welds (P4C), on the 110° and 290° azimuth downcomers. Repairs comprised of mechanical clamping devices, one on each elbow, were installed prior to start up from the D3R13 outage. Because these clamping devices concealed several welds and would have prevented their inspection, the devices were removed during the D3R14 refueling outage to provide access to the welds for the automated ultrasonic scanner. All four of the downcomers were then inspected using qualified automated ultrasonic methods to the extent possible.

The internal core spray ultrasonic examinations conducted during the D3R14 identified and sized the two existing flaws in the downcomer pipe to lower elbow welds (P4C), on the 110° and 290° azimuth downcomers. Three previously undetected flaws were also identified and sized in the shroud penetration thermal sleeve collar near the P8a welds. These flaws were initially observed during the ultrasonic examination and flagged as "suspect" areas and were later verified with enhanced visual examination. All three of the shroud pipe to collar flaws are located in the collar side of the weld approximately 0.50" back from the face of the collar. The flaws are located on the 80°, 110° and 260° downcomers. Specific details of the component geometry and the flaw locations are as depicted in Figure 3.1 through 3.5.

The main analytical approach used here to justify continued operation is a limit load analysis which only requires primary loads in the evaluation. However, additional sensitivity studies were also performed in which secondary loads from the thermal, seismic and LOCA events are included. The loads used to evaluate these flaws were developed from a piping analysis model of the Dresden Core Spray system. As a result of the significant indications present in the 80° collar, the piping analysis model was modified to consider the increased flexibility at this point. This report provides the assessment criteria, design inputs and results for the various evaluations performed to evaluate the impact on these flaws on the safe operation of the plant.

Section 3 of this report provides a summary of the method and extent of the examinations performed as well as a detailed definition of the indications identified. Section 4 provides the materials evaluation with an assessment of the root cause and definition of material properties and the crack growth rate used in the flaw evaluation. The definitions of the loading cases and load combinations used are provided in Section 5. A detailed description of the core spray line modeling and analysis along with a summary of the results is provided in Section 6. The flaw structural integrity and leakage evaluations are provided in Sections 7 and 8, respectively. Section 9 provides a description of the core spray system LOCA evaluation. Failure assessments and loose parts evaluation are provided in Section 10 and 11, respectively. A summary of the results and conclusions is provided in Section 12, while the references are presented in Section 13.

Figure 2.1 - Core Spray Piping Inside the RPV Annulus

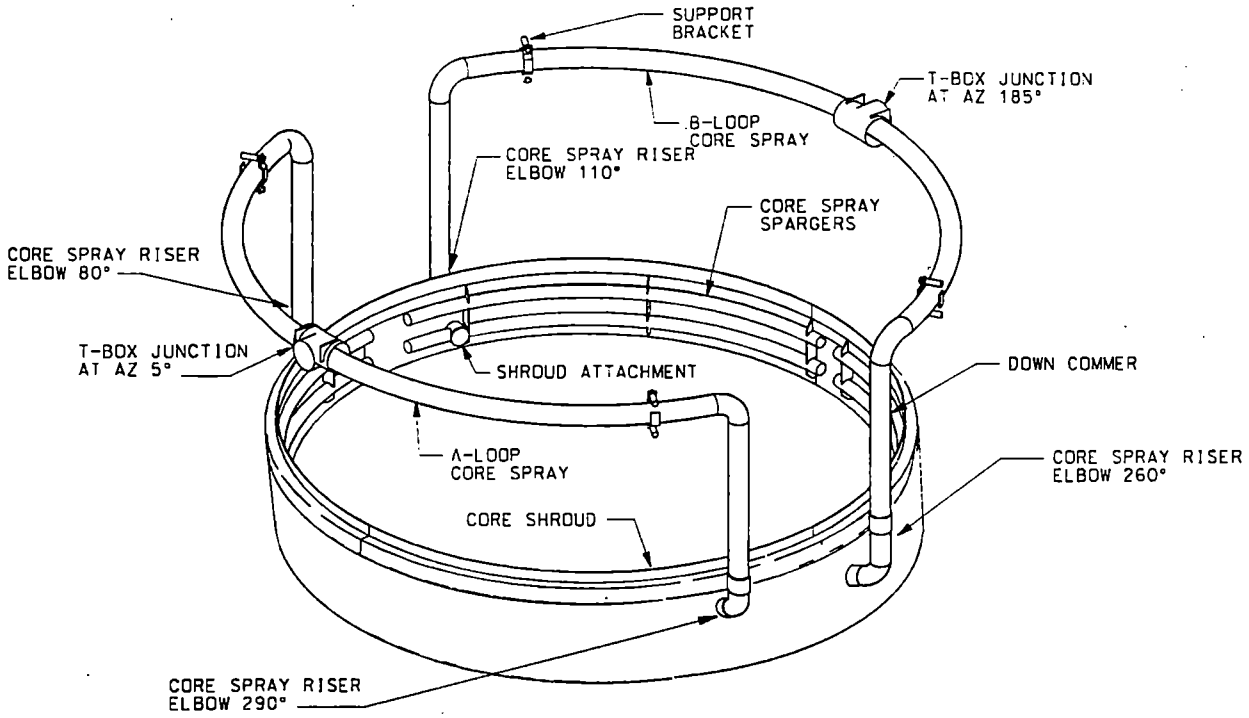

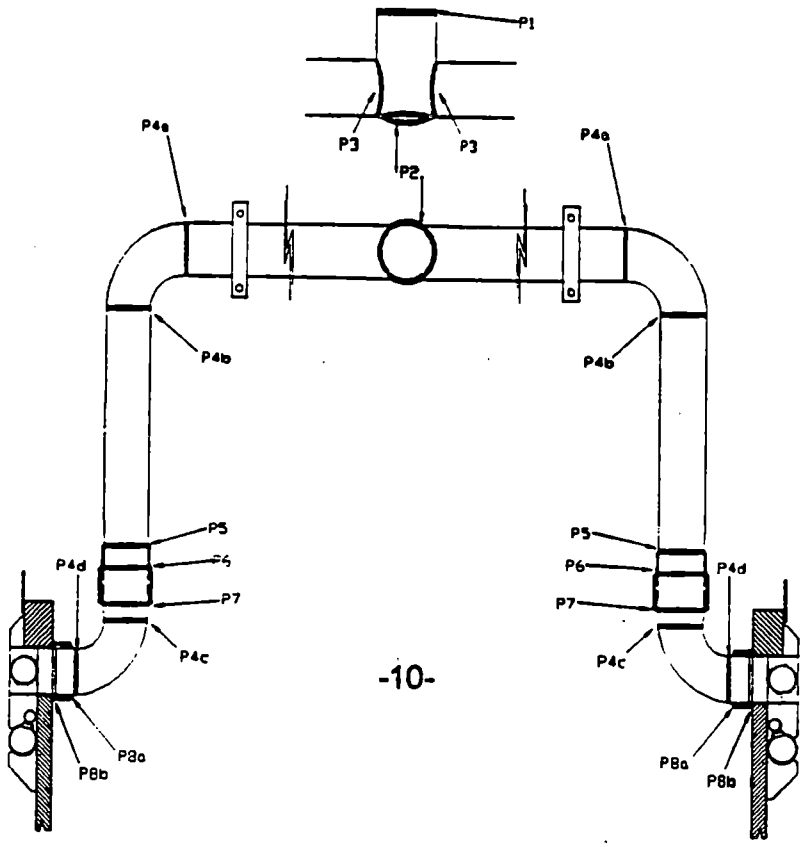

3.0 DESCRIPTION OF INDICATIONS

3.1 Examination Description

The internal core spray examinations conducted during the Dresden Unit 3 D3R14 refueling outage (References 4 and 5) were performed in accordance with the "BWR Core Spray Internals Inspection and Evaluation Guidelines" (BWRVIP-18), Reference 12.

The primary examination system utilized for the examination of the core spray piping welds was the GE automated core spray inspection tool (CSI-2000), which is a computer controlled multi-axis robotic inspection tool. This system employs an automated ultrasonic scanning head which contains both 60° and 70° shear wave search units. NDE technique and tool position uncertainty demonstrations for this system were performed at the EPRI NDE Center in accordance with the criteria established in BWRVIP-03, Reactor Pressure Vessel and Internals Examination Guidelines.

Additionally, where access restrictions prevented 100% ultrasonic coverage of a given weld, supplemental enhanced visual examination (EVT-1) was performed to ensure 100% coverage of the weld, where possible. Enhanced visual examination was also performed on the elbow to shroud pipe welds (P4d) and the shroud pipe to collar welds (P8a), because the ultrasonic techniques employed at these locations have not yet been fully qualified per BWRVIP-03, Reactor Pressure Vessel and Internals Examination Guidelines.

Finally, internal to the shroud, enhanced visual examinations were performed on the core spray sparger tee-box cover plate welds, sparger to tee-box branch connection welds and sparger end cap welds. Also, modified VT-1 (MVT-1) examinations were performed on the sparger nozzles, piping and brackets.

3.2 Core Spray 80° Collar Weld IP8a

This collar (Figure 3.1) has three approximately collinear flaws, for a total length of 235° or 16.4 inches. The first segment extends from 275° to 345°, reappears at 355° to 80°, and then reappears again at 100° extending to 150°. Penetration collars are referenced to zero degrees at top center and clockwise viewing the shroud from the annulus side. The collars have an outside diameter of 8 inches and a circumference of 25.1 inches. The UT interrogation covered 100% of this weld which was also examined visually.

3.3 Core Spray 110° Lower Elbow to Downcomer Pipe Weld 2P4c

The elbow flaw (Figure 3.2) is in the elbow side of the upper pipe to elbow weld starting at 244° and extending to 324° for a length of 4.6 inches or 80°. Elbows are referenced zero degrees to the vessel wall and clockwise viewed in the direction of flow. The UT interrogation covered 100% of this weld.

3.4 Core Spray 110° Collar Weld 2P8a

This collar (Figure 3.3) flaw starts at 294° and extends to 16° for a length of 82° or 5.7 inches. The UT interrogation covered 100% of this weld which was also examined visually.

3.5 Core Spray 260° Collar Weld 3P8a

This collar (Figure 3.4) flaw starts at 277° and extends to 36° for a total of 119° or 8.3 inches. The UT interrogation covered 100% of this weld which was also examined visually.

3.6 Core Spray 290° Lower Elbow to Downcomer Pipe Weld 4P4c

The elbow flaw (Figure 3.5) starts at 208° and extends to 286° for a total length of 4.5 inches or 78°. The UT interrogation covered 100% of this weld.

3.7 Crack Growth Length

The flaw lengths as determined by ultrasonic examinations were increased by a crack growth length to establish an evaluated flaw length (EFL). A crack growth length for an evaluation period of 48 months of hot operation with a 100% availability factor was added to both ends of the flaw. A summary of the evaluated flaw lengths is provided below.

Table 3.1 Summary of Flaw Lengths

Flaw Location	Weld	Measured Flaw Length (inches)[1]	Crack Growth Length per Cycle (inches)[2,3]	1 Cycle Evaluated Flaw Length (inches)[4]	2 Cycle Evaluated Flaw Length (inches)[5]
80° Downcomer Collar	1P8a	16.4	0.865	18.14	19.87
110° Downcomer Elbow	2P4c	4.6	0.865	6.33	8.06
110° Downcomer Collar	2P8a	5.7	0.865	7.43	9.16
260° Downcomer Collar	3P8a	8.3	0.865	10.03	11.76
290° Downcomer Elbow	4P4c	4.5	0.865	6.23	7.96

Notes:

1. Measured lengths are the results obtained from UT examinations with linear lengths calculated using the outside diameter.

2. 5.00×10^{-5} inches per hour represents an upper bound limit for IGSCC crack growth in ductile materials (Reference 13).

3. Crack growth per cycle is based on a twenty-four month 100% availability cycle (24x30x24=17,280 hours).

4. One Cycle Evaluated Flaw Length (EFL) = Measured Length + 2(CGL)

5. Two cycle Evaluated Flaw Length (EFL) = Measured Length + 4(CGL)

Figure 3.1 - Core Spray A-Loop 80 Upper Sparger Inlet Collar

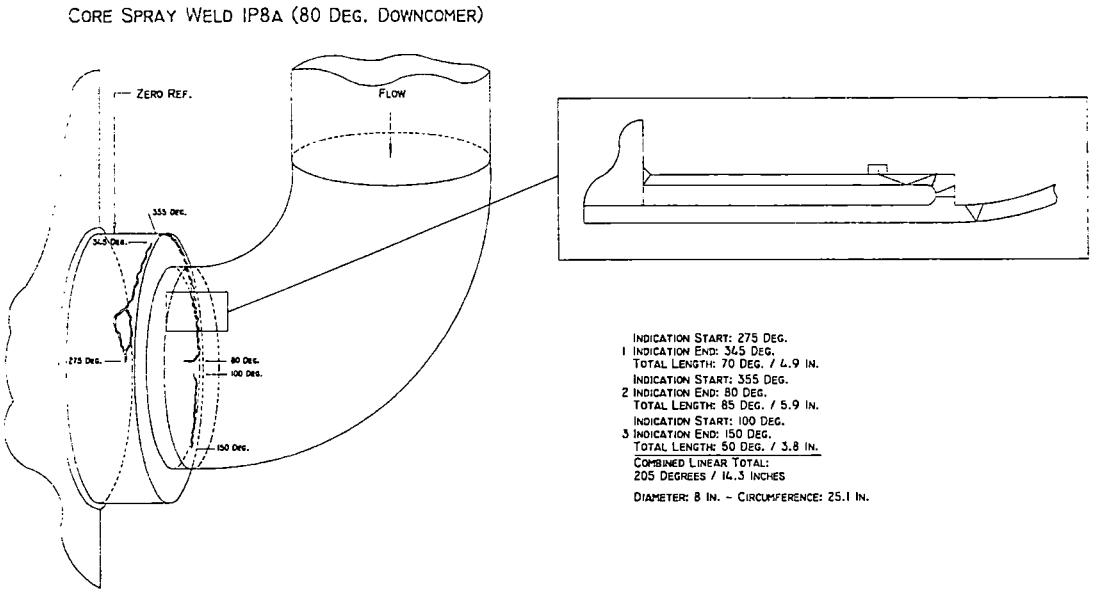

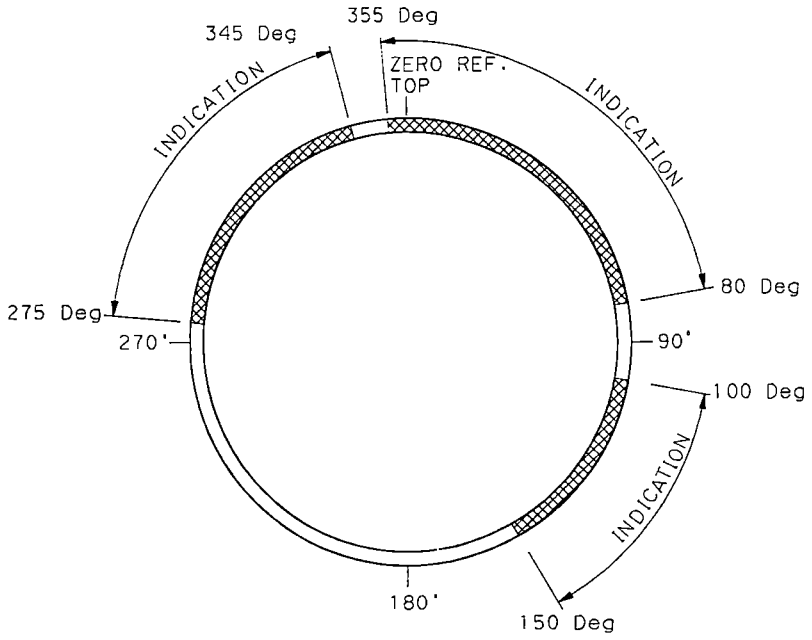

Figure 3.2 - Core Spray B-Loop 110° Lower Sparger Inlet Elbow

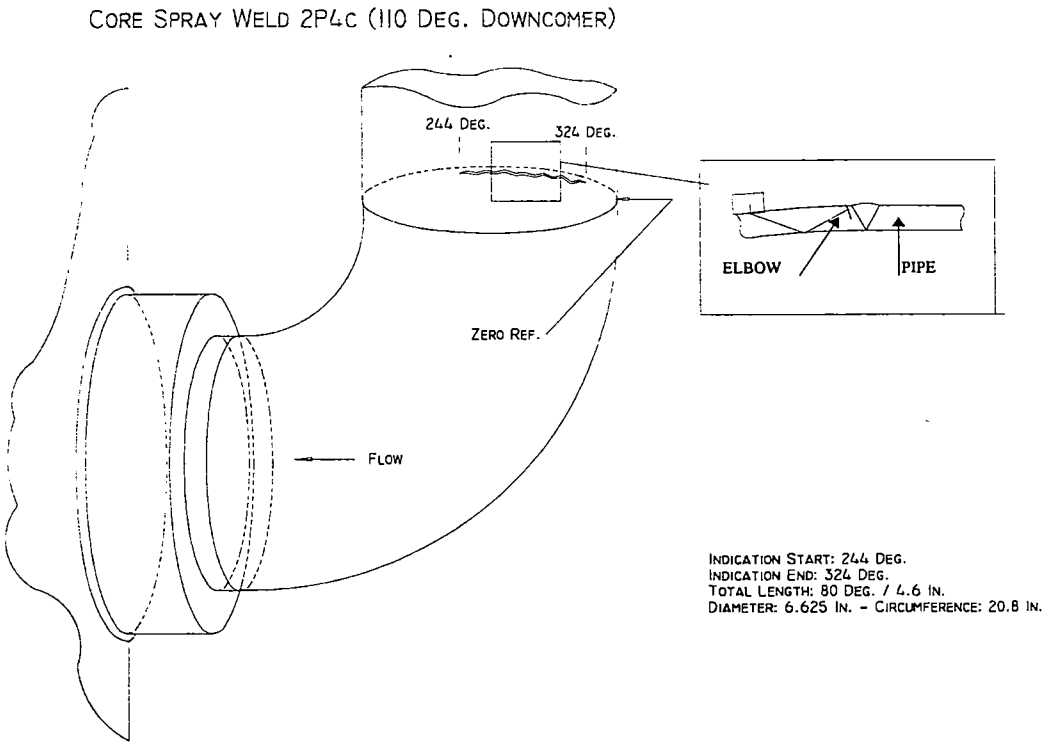

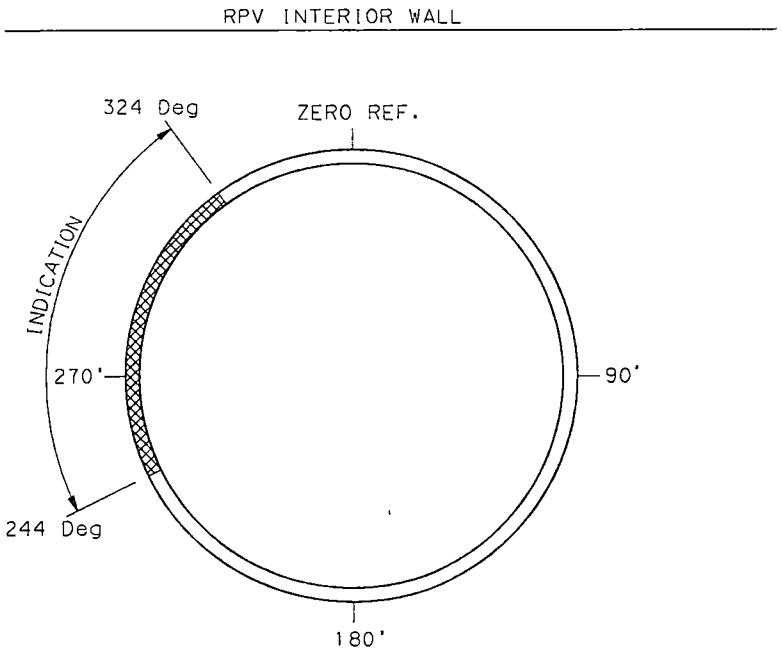

Figure 3.3 - Core Spray B-Loop 110° Lower Sparger Inlet Collar

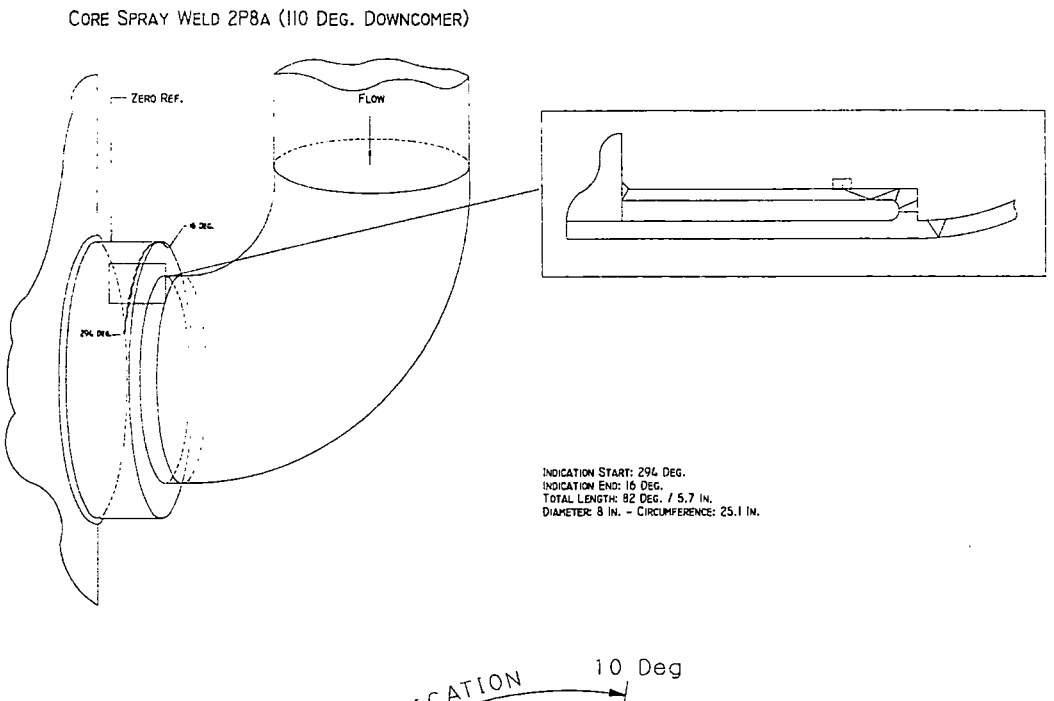

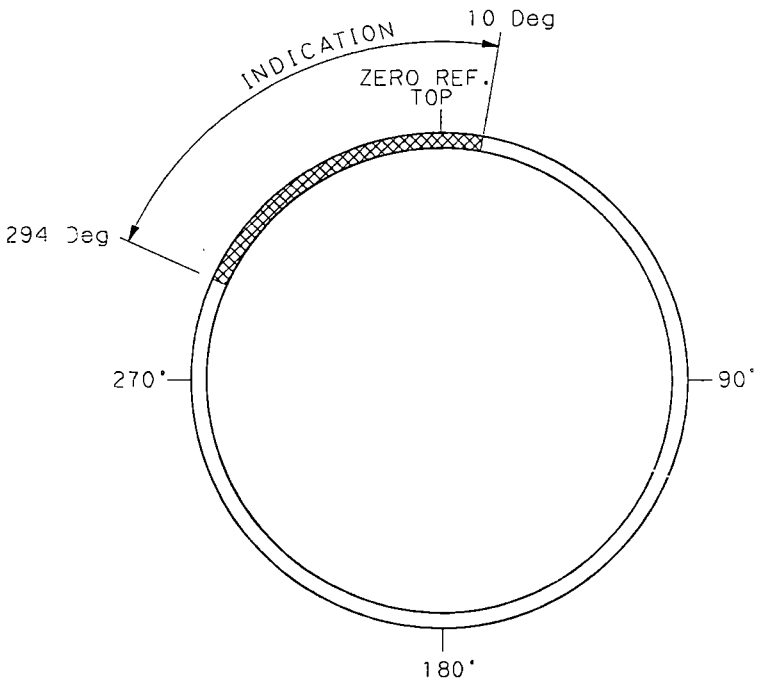

Figure 3.4 - Core Spray B-Loop 260° Lower Sparger Inlet Collar

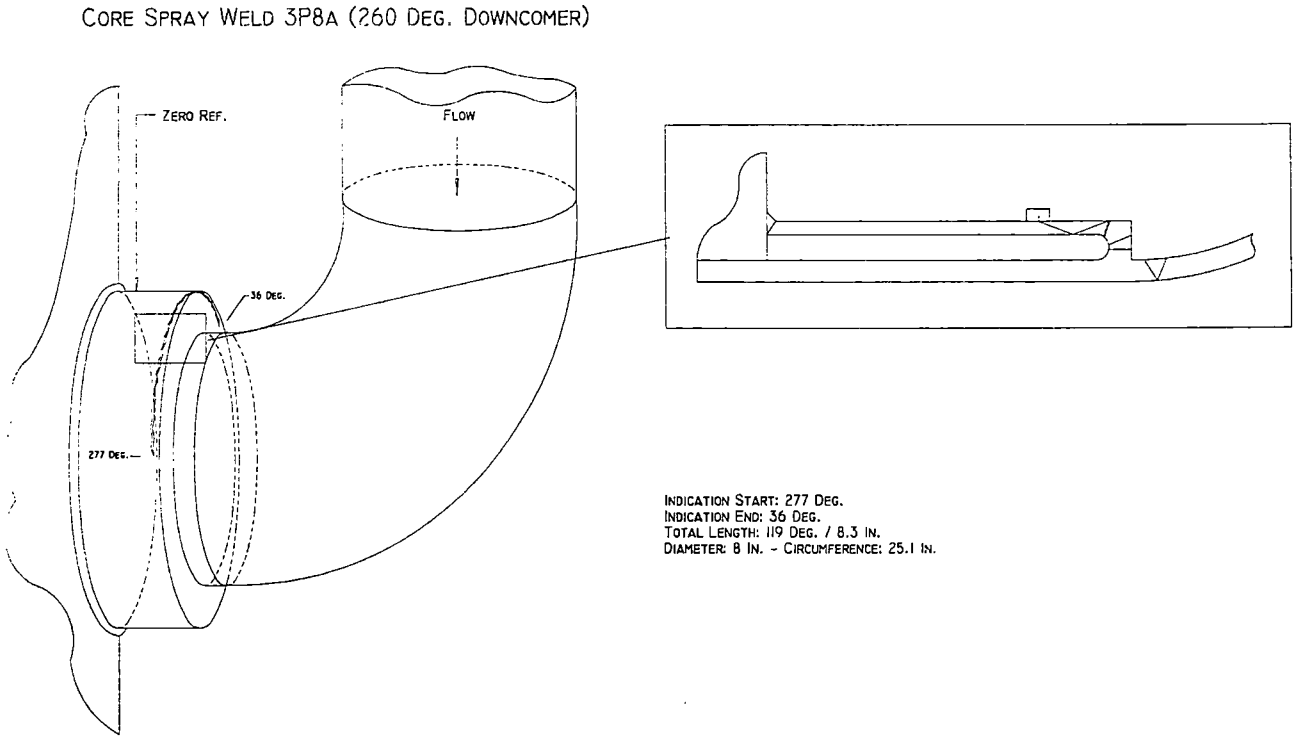

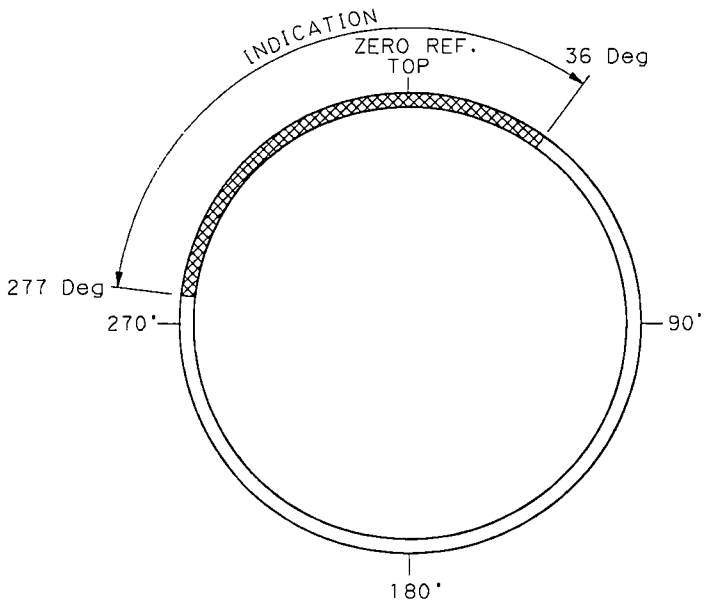

Figure 3.5 - Core Spray A-Loop 290° Upper Sparger Inlet Elbow

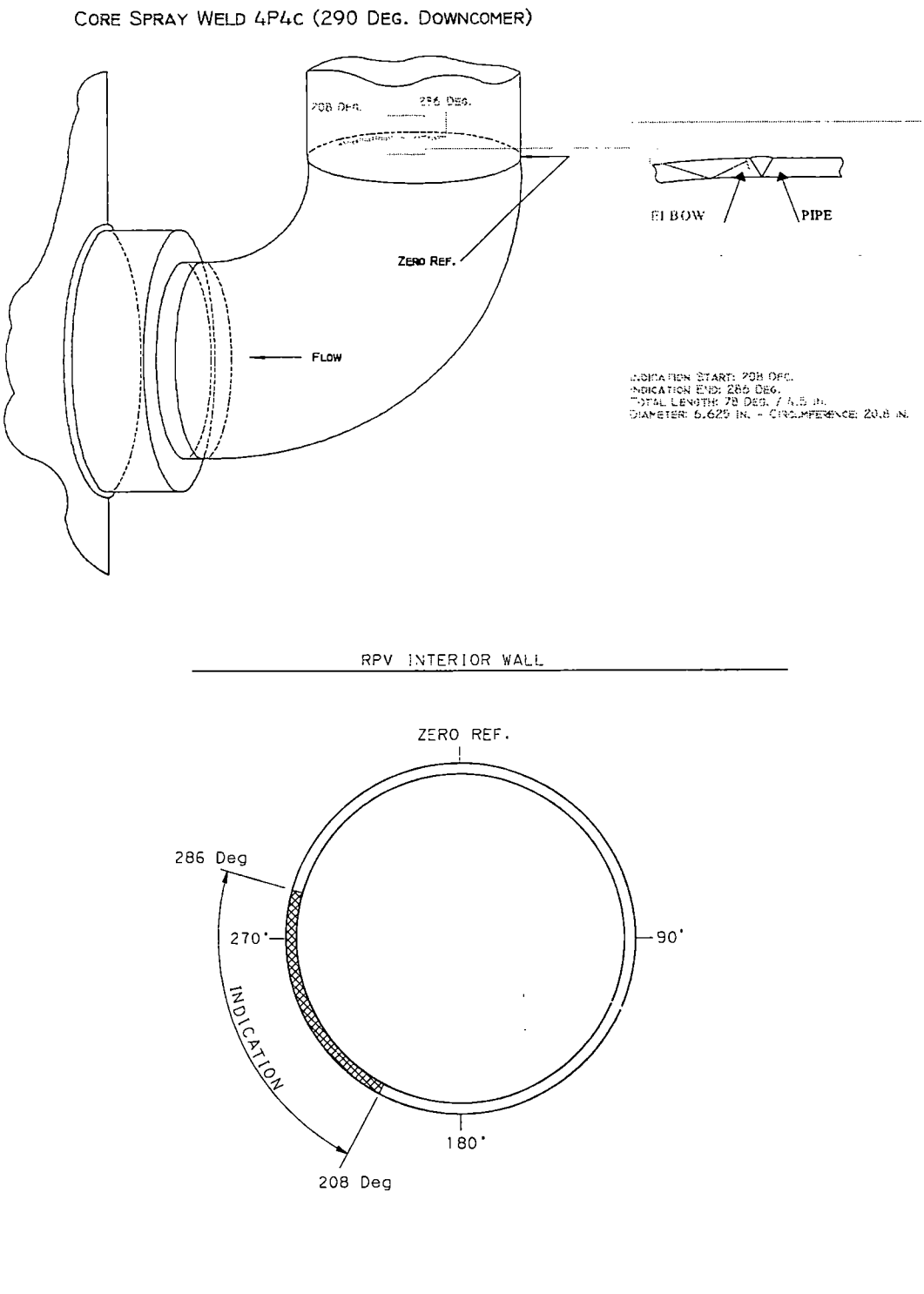

4.0 MATERIALS EVALUATION

4.1 Overview

Indications were found in the Heat Affected Zones (HAZ) of the 80°, 110° and 260° collar / thermal sleeve assembly circumferential welds(P8a) and in the 110° and 290° lower downcomer elbow circumferential welds (P4c) of the core spray piping in the RPV annulus area (see Figure 2.1). These locations are consistent with Intergranular Stress Corrosion Cracking (IGSCC) susceptability requirements. This particular degradation mechanism is well documented for stainless steel components exposed to the high temperature reactor water of BWRs. Several other BWRs including Dresden 2 and Dresden's sister plants Quad-Cities Units 1 and 2, have reported core spray piping cracks which were identified as IGSCC.

4.2 Fabrication

The General Electric Company (GE) design specifications as well as the fabricator records (Willamette) have been reviewed, References 17 through 22. All of the components are fabricated from solution heat-treated Type 304 austenitic stainless steel ASTM A-403, Grade WP-304 and ASTM A-276, Type 304. From a review of the fabrication records, the weld processes used to perform weld P8a for the collar assembly included Gas Tungsten Arc Weld (GTAW) for the root and Shielded Metal Arc Weld (SMAW) for the balance using E(ER)308 filler. The fracture toughness and tensile properties of the base material (collar) were used for the flaw analysis since the flaw originates in the HAZ of the collar adjacent to and not within the weld root. The weld process employed for the pipe to elbow fabrication was GTAW.

4.3 Crack Growth Rate

The principle driving force propagating IGSCC cracks comes from the weld residual stresses, because the applied loads during normal operation are insignificant. The residual stresses are self-relieving and will diminish as the crack extends. As the stress intensity factor at the tip of the growing crack drops below the threshold stress intensity for IGSCC (K_{IGSCC}), crack extension will stop. Therefore, the existing crack will propagate only as long as the

residual stress field is sufficiently high to support crack propagation. These arguments suggest that a lower IGSCC crack growth rate may be justified. However, ComEd has used the currently accepted bounding crack growth rate of $5x10^{-5}$ inches/hour (Reference 13).

4.4 Material Behavior

The ductile or brittle response of the material of cracked core spray components is evaluated with respect to initial characteristics and environmental degradation. All of the materials used in fabrication, were austenitic stainless steels as indicated in Section 4.2 of this report. These materials do not undergo phase transformation during thermal processing. The most significant material response to thermal processing is grain boundary precipitation of chromium carbides, and this response produces a zone adjacent to the grain boundaries that is depleted in chromium. This condition is termed sensitization and can be produced during welding. This condition influences the electrochemical response of the material (increasing susceptibility to IGSCC), but does not alter the ductility or toughness of the material.

Exposure of austenitic stainless steels to irradiation can lead to a loss of ductility and an increased sensitivity to Irradiation Assisted Stress Corrosion Cracking (IASCC). The onset of IASCC occurs at approximately $5x10^{20}$ n/cm^2. The neutron fluence in the area of the core spray is less than the threshold limit, therefore, no reduction in toughness or increased sensitivity to IASCC is expected.

4.5 Conclusion

In conclusion, the cracking observed in the core spray system is the result of IGSCC in austenitic stainless steels. The stresses driving the cracking are residual stresses (self relieving) indicating that the rate of crack growth will slow as cracking proceeds through wall. Therefore, the crack growth rate of $5x10^{-5}$ inches/hour represents a conservative upper bound limit. In addition, the material properties of the core spray system will remain ductile throughout the life of the system.

5.0 LOAD DEFINITIONS AND LOAD COMBINATIONS

5.1 Load Cases

The load definition and load combinations described in the following subsections are in agreement with the design basis requirements of the Dresden UFSAR, Reference 23, and are consistent with the BWRVIP recommendations, Reference 12. An additional load combination not required in the design basis for Dresden was also evaluated. The simultaneous occurrence of a safe shutdown earthquake, SSE and a design basis accident, DBA, LOCA was postulated.

DWGT = Dead Weight
TH01 = Thermal 1 Normal Operation
TH02 = Thermal 2 Feedwater Transient
TH03 = Thermal 3 Core Spray - DBA Short Term (DBA1)
TH04 = Thermal 4 Core Spray - DBA Intermediate Time Frame (DBA2)
TH05 = Thermal 5 Core Spray - DBA Long Term (DBA3)
TH06 = Thermal 6 Core Spray - ADS Blowdown, small and intermediate breaks
TH07 = Thermal 7 HPCI Event - No Core Spray
P_1 = Pressure 1 (Internal Piping Pressure - No Injection = 0 psid)
P_2 = Pressure 2 (Internal Piping Pressure - Injection at 4500 gpm = 45 psid)
P_3 = Pressure 3 (Internal Piping Pressure - Injection at 5650 gpm = 71 psid)
DWH1 = Drag Load 1 (External Drag Loads on the Pipe Surface - Normal Flow)
DWH2 = Drag Load 2 (External Drag Loads on the Pipe Surface - Recirculating Line Break Flow)
DWH3 = Drag Load 3 (External Drag Loads on the Pipe Surface - Main Steam Line Break Flow)
OBDX = X Direction OBE Differential Seismic Displacement
OBDZ = Z Direction OBE Differential Seismic Displacement
OBDY = Y Direction OBE Differential Seismic Displacement
OBE1 = OBE Response Spectra Analysis
SSDX = X Direction SSE Differential Seismic Displacement (2 x OBDX)
SSDZ = Z Direction SSE Differential Seismic Displacement (2 x OBDZ)

SSDY = Y Direction SSE Differential Seismic Displacement (2 x OBDY)
SSE2 = SSE Response Spectra Analysis
SDIS = RRLB Core Shroud Displacement
INJF = Core Spray Injection Force

5.1.1 Dead Weight (DWGT)

The core spray piping from the RPV nozzle to the shroud penetrations consists of 6" nominal Outside Diameter (OD) schedule 40 pipe and 8" nominal OD schedule 40 pipe. The piping is normally below the water level except for a LOCA event. In a LOCA event, the water level may drop below the core shroud penetrations. The weight of water contained inside the piping is included and the buoyancy force is conservatively neglected.

5.1.2 Thermal Expansion & Pressure Loads (TH01-06, PZER & PDES)

The radial and longitudinal differential thermal expansions of the RPV and the shroud are included in the thermal expansion analyses for the core spray piping. The radial dilation of the RPV under internal pressure is also considered for each thermal mode. Calculations for thermal displacements at support locations are documented in Section 1 and thermal mode definitions are in Section 2 of Reference 2.

Definition of Thermal Modes

Mode	Title	Pipe	RPV	Shroud	Annulus Water Temp.	RPV (psig)
1	NORM Oper	522	522	536	522	1050
2	FW TRANS	300	522	433	300	1050
3	CS-DBA1	195	522	536	270	27
4	CS-DBA2	195	522	270	270	27
5	CS-DBA3	179	232	232	232	7
6	CS-ADS	209	522	298	298	50
7	HPCI-NOCS	366	522	366	366	150

Normal Condition (TH01)

Temperature within the annulus region of the RPV is 522°F which is the temperature of Region B as specified in the Reactor Thermal Cycles diagram (Reference 3). The temperature of the shroud (536°F) is taken as the average temperature of the annulus region (522°F) and core region water temperature (550°F). Core spray piping temperature is the same as the temperature of Region B.

Feedwater Transient Condition (TH02)

A Loss Of Feedwater Pumps (LOFP) is considered for upset conditions. In this event, the water temperature in the annulus region is dropping rapidly to 300°F while the temperature of the RPV remains at the normal operating temperature of 522°F. The average temperature of the shroud under this transient condition is 433°F. The temperature of the core spray piping is considered to be the temperature of the water in the annulus region.

Core Spray (THO3) - DBA Short Term (CS-DBA1)

This mode describes the condition shortly after core spray is initiated due to a Design Basis Accident (DBA) recirculation line break. The reactor has depressurized to 27 psig. Cold core spray water (120°F) is injecting, cooling the piping while the RPV and core shroud remain hot (522°F and 536°F, respectively). The pipe temperature is estimated as the average of the core spray water temperature and the annulus water temperature (270°F) which is based on T_{SAT} at 27 psig reactor pressure.

Core Spray (THO4) - DBA Intermediate Term (CS-DBA2)

This mode describes the condition in CS-DBA1, but at a later time when the core shroud has cooled along with the piping. Since the RPV cools much more slowly than the core shroud, it is assumed to remain at its normal operating temperature (522°F) as a bounding condition. Core shroud temperature is based on T_{SAT} at 27 psig which is 270°F. The piping temperature is the same as in CS-DBA1.

Core Spray (TH05) - DBA Long Term (CS-DBA3)

This mode describes the condition at a later time than CS-DBA2 (≈ 6 hrs after accident) when the RPV has cooled along with the core shroud and piping. The reactor pressure has decreased to 7 psig with T_{SAT} = 232°F annulus water temperature and 125°F core spray water.

Core Spray (TH06) - ADS Blowdown for Small or Intermediate Breaks

This mode describes a bounding condition for the case of a small or intermediate break in which the ADS system depressurizes the vessel to allow the core spray and LPCI systems to operate. The ADS relief valves close at a pressure of 50 psig so this pressure is used as a minimum for this event. The bounding thermal condition is judged to be the point at which the core shroud and piping temperature have cooled and the RPV remains hot. Core shroud temperature is based on T_{SAT} at 50 psig which is 298°F. RPV temperature is analyzed as 522°F. Piping temperature is based on the average of 120°F core spray water and 298°F annulus water temperature.

HPCI (TH07) - Unassisted HPCI Event, No Core Spray

This mode is for a small break event in which the HPCI system operates alone to maintain reactor water level. The minimum operating reactor pressure for HPCI is 150 psig. This pressure is used as a basis for the minimum reactor annulus water temperature, T_{SAT} = 366°F. The bounding thermal condition for this event is the point where the core shroud and piping have cooled while the RPV remains hot. The core shroud and piping are analyzed at the annulus temperature of 366°F and the RPV at 522°F.

5.1.3 Drag Load (DWH1, DWH2, DWH3)

The drag load of the reactor water on the core spray piping is evaluated in the normal operating condition (DWH1) and during a Reactor Recirculation Line Break (RRLB) condition (DWH2). The drag loads during an RRLB were found to envelope those of a Main Steam Line Break (DWH3). Drag load calculations are provided in Section 21 of Reference 9.

5.1.4 Core Spray Injection Force (INJF)

Since the thermal sleeve in the core spray RPV nozzle is a slip joint and not welded to the nozzle, the hydraulic force of the water is applied externally to the core spray piping at the 8" x 6" Tee-box in the axial direction of the 8" diameter thermal sleeve. The force is based on the maximum core spray system flow rate.

5.1.5 Displacement Analyses (OBDX, OBDZ, SSDX, SSDZ, SDIS)

The core spray piping is anchored to the core shroud at Node Points (NP) 307 and 327 as shown in Figure 6.1. It is attached to the RPV by supports located at node points 75, 125, 145 and 195. Displacement of the core shroud relative to the RPV results in differential support motion which is analyzed for OBE and SSE seismic events as well as for the RRLB events.

The OBE seismic core shroud displacements are 0.29" in the N-S direction and 0.35" in the E-W direction (Reference 1, Section 10). SSE displacements are twice the OBE displacements.The seismic displacements are analyzed separately in the X and Z-directions (X = east-west axis, Z = north-south axis). The vertical Y displacements are negligible. Since the SSE seismic displacements are twice the OBE displacements, only the OBE is analyzed and the results are doubled to obtain the SSE results.

The RRLB event was determined to bound the MSLB event with respect to loads on the core spray piping. It was analyzed by calculating the cracked shroud displacement in the direction of each recirculation suction nozzle at 155° and 335°.

5.1.6 Seismic Inertial Analyses (OBE1, SSE2)

OBE 1% damping and SSE 2% damping were used in the piping analyses. Two spectra, one at the RPV penetrations and one at the core shroud penetrations are enveloped for this analysis.

A uniform acceleration of .08g's (OBE) and .16g's (SSE) was used in the vertical Y-direction for all frequencies. The maximum of the X+Y or Y+Z combined seismic responses are used. The X-direction and Z direction seismic

displacement results are combined separately with the inertial seismic and the two combinations are enveloped. Y-direction seismic displacements are negligible. The contributions of residual modal mass, hydrodynamic mass and the gap type supports are included in the analysis results.

Additional Analysis Notes

For the 6" diameter piping the normal drag force is in the same direction as the weight. Since the buoyancy force acts in the opposite direction of the drag force and weight, the bouyancy force is conservatively not included.

For Thermal Mode 1 and RRLB Drag load, the piping moves toward the gap at the bracket supports at NP's 125 and 145. The free displacements at the supports are input at NP's 125 and 145 in the final Thermal Mode 1 and RRLB drag analyses so that the supports do not take a load in the gap direction.

5.2 Load Combinations For Limit Load Flaw Evaluations

Load Comb No.	Service Level	Combination
1	A	DWGT+ DWH1
2	A	DWGT+ DWH1+ TH01
3	B	DWGT+ DWH1+ TH02
4	B	DWGT+ DWH1+ OBDX+ OBE1
5	B	DWGT+ DWH1+ OBDZ+ OBE1
6	B	DWGT+ TH01+ DWH1+ OBDX+ OBE1
7	B	DWGT+ TH01+ DWH1+ OBDZ+ OBE1
8	C	DWGT+ TH03+ DWH1+ INJF
9	C	DWGT+ TH04+ DWH1+ INJF
10	C	DWGT+ TH05+ DWH1+ INJF
11	C	DWGT+ TH06+ DWH1+ INJF
12	C	DWGT+ TH07+ DWH1
13	C	DWGT+ DWH1+ SSDX+ SSE2
14	C	DWGT+ DWH1+ SSDZ+ SSE2
15	C	DWGT+ TH01+ DWH1+ SSDX+ SSE2
16	C	DWGT+ TH01+ DWH1+ SSDZ+ SSE2
17	C	DWGT+ DWH2+ SDIS
18	C	DWGT+ TH01+ DWH2+ SDIS
19	D	DWGT+ DWH2+ SDIS+ SSDX+ SSE2
20	D	DWGT+ DWH2+ SDIS+ SSDZ+ SSE2
21	D	DWGT+ DWH2+ SDIS+ SSDX+ SSE2+ TH01
22	D	DWGT+ DWH2+ SDIS+ SSDZ+ SSE2+ TH01
23	D	DWGT+ TH03+ DWH1+ INJF+ SSDX+ SSE2
24	D	DWGT+ TH03+ DWH1+ INJF+ SSDZ+ SSE2
25	D	DWGT+ TH04+ DWH1+ INJF+ SSDX+ SSE2
26	D	DWGT+ TH04+ DWH1+ INJF+ SSDZ+ SSE2
27	D	DWGT+ TH05+ DWH1+ INJF+ SSDX+ SSE2
28	D	DWGT+ TH05+ DWH1+ INJF+ SSDZ+ SSE2
29	D	DWGT+ TH06+ DWH1+ INJF+ SSDX+ SSE2
30	D	DWGT+ TH06+ DWH1+ INJF+ SSDZ+ SSE2
31	D	DWGT+ TH07+ DWH1+ SSDX+ SSE2
32	D	DWGT+ TH07+ DWH1+ SSDZ+ SSE2

Load Combinations For Leakage Evaluations:

Load Comb No.	Service Level	Combination
1	C/D	DWGT + TH04 + P_2
2	C/D	DWGT + TH04 + P_3

6.0 CORE SPRAY PIPING MODELLING AND ANALYSIS

6.1 Piping Models

The purpose of this piping analysis is to provide forces and moments on the 6" diameter core spray piping in the reactor annulus to be used for evaluation of flaws found in the pipe elbows and in the collars at core shroud penetrations. The subject piping was analyzed using the PIPSYS and GAPP programs for the load conditions described in Section 5.0. The affected portion of the piping representing the upper and lower core spray spargers was analyzed utilizing two separate models delineated as the "upper sparger" and "lower sparger".

The piping models are based on the design basis drawings (References 17 through 22) and are shown in Figure 6.1. These models consist of core spray piping inside the annulus. From the 8" RPV nozzle and 8"x6" tee-box, the 6" piping follows the circumference of the reactor above the core shroud to two vertical legs which drop down and penetrate the core shroud horizontally after a 90° elbow. The model ends at these anchored shroud penetrations, NP 307 and NP 327. The piping is supported directly to the RPV at NP's 75, 125, 145, and 195.

This core spray piping exists in mirror image on both sides of the reactor, with the only difference being that the 'B' loop downcomers drop to a lower elevation on the core shroud to connect with the lower core spray sparger. The piping model for the lower sparger was modified by shortening the vertical legs to create the upper sparger model. Since the two piping systems are 180° apart, the coordinate systems used in the models point in opposite spatial directions for the two models. The isometric drawing in Figure 6.1 shows the appropriate coordinate systems. The piping is 6" schedule 40, TP-304 stainless steel with a short leg of 8" schedule 40, TP-304 piping at the reactor nozzle. Flexible anchors are modeled at the core shroud penetrations with the model terminating at the 6" 90° elbow outlet. Stiffnesses for the shroud penetration assembly were calculated based on the finite element analysis of the shroud penetration thermal sleeve and sparger tee-box, as described in Reference 9. The 8"x6" tee-box is modelled as 8" Sch. 40 piping.

A third model was developed, Figure 6.2, which includes the sparger piping and supports inside the shroud for the Loop A upper sparger 80° downcomer. This model was developed to determine the piping and support loads based on the increased flexibility caused by the extensive collar crack. Although the 80° collar has been demonstrated to remain intact (Reference 1, Section 5), the most limiting models for load generation in the piping and supports are to consider the collar completely intact (i.e., an anchor point) and free rotationally (i.e., unable to carry any moment loads). This model restricts translations but not rotation because the sparger tee box piping is supported inside the shroud as shown in Figure 6.3. Translation in the vessel radial direction is restricted by the collar fracture face in the annulus, and by the tee-box gusset inside the shroud. The vertical and horizontal translations are restricted by the close fit between the pipe and shroud penetration. The results of these different limiting models, Reference 1, were reviewed and the greatest loads used in the flaw evaluations.

Additionally, the change in natural frequencies between the rigid and flexible piping models was examined to ensure flow induced vibration would not be a concern during normal operation. The natural frequency of the rigid model is 29.8 hz and 27.8 hz for the flexible model. The vortex shedding frequency during normal operation was determined to be 3.3 hz in Section 11 of Reference 2 and thus the natural frequency is far removed from the vortex shedding frequency. Consequently, the change in frequency will not have a significant affect on the magnitude of flow induced vibration.

Figure 6.1 - Core Spray Piping Analysis Model

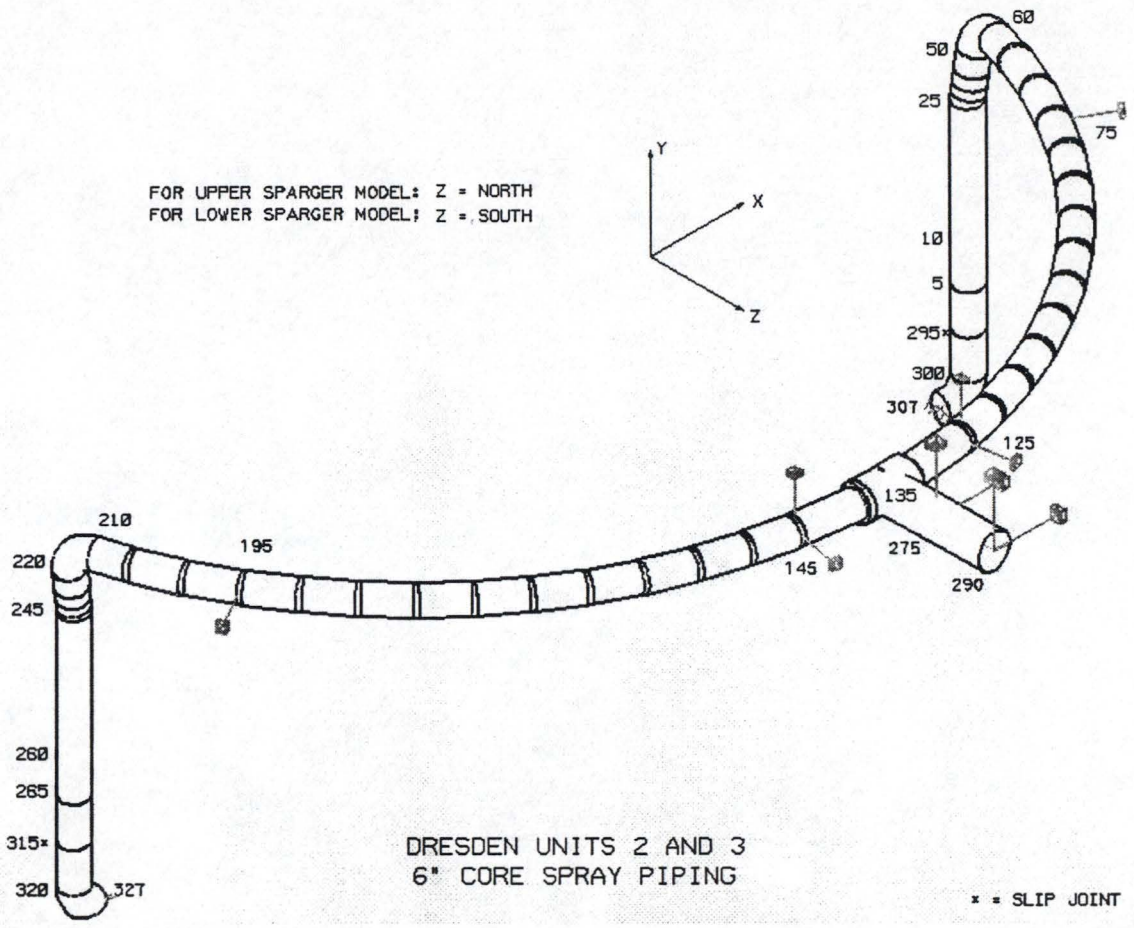

Figure 6.2 - Core Spray Loop A Piping Analysis Flexible Model

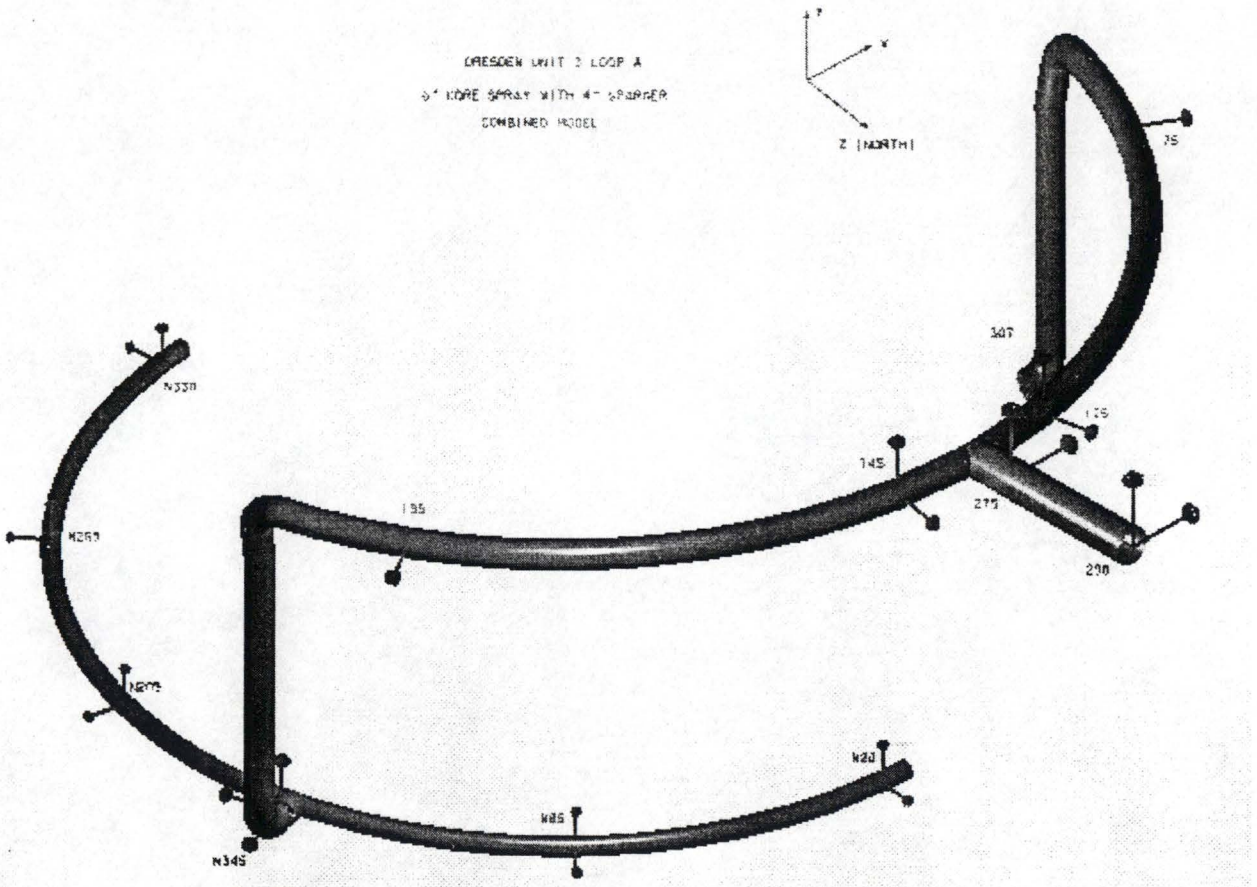

Figure 6.3 - Sparger Tee-Box Finite Element Model

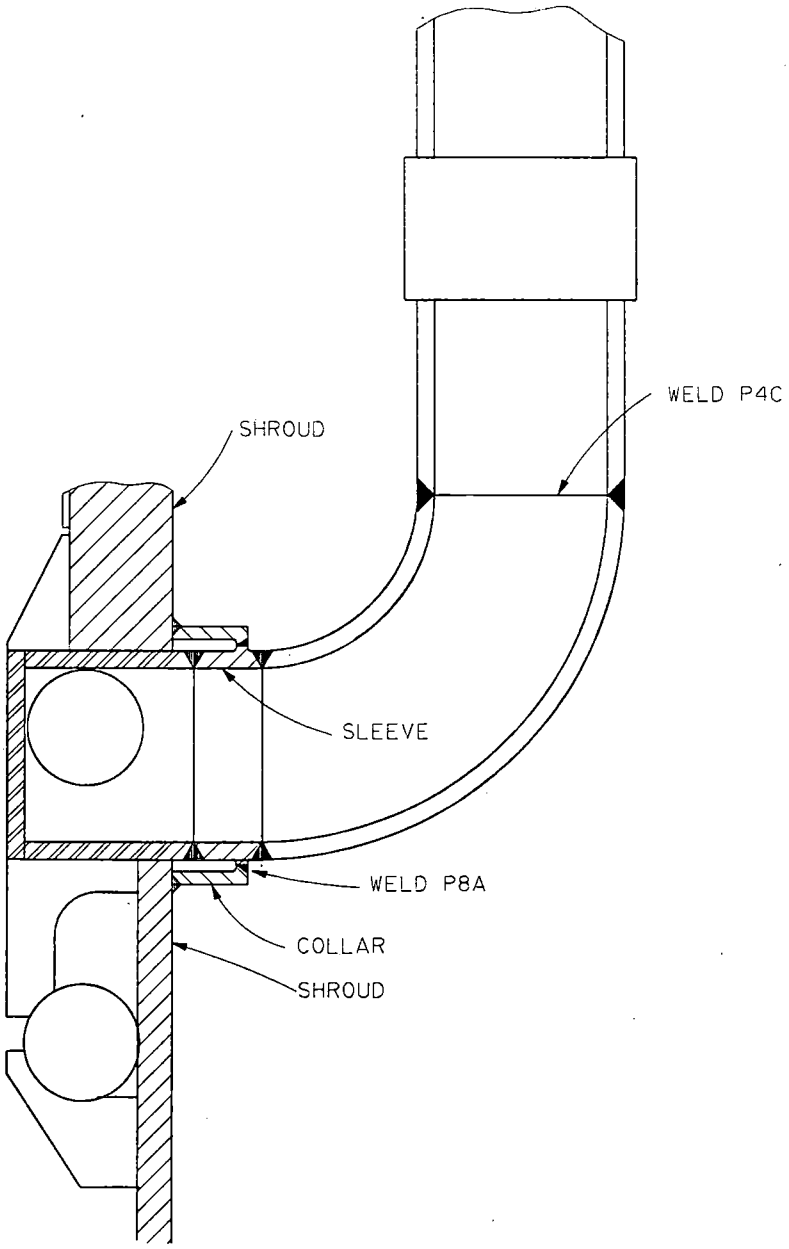

7.0 FLAW EVALUATIONS

This section describes the methodology, details and results of the Core Spray flaw assessment for each of the four flaws. The material, loading and stress analysis results as defined in Sections 4, 5 and 6 serve as the primary inputs for these flaws evaluations. The flaw evaluations were performed using the ASME Section XI, Appendix C, limit load method for the flaws as characterized in Section 3. Provided below is a summary of the evaluations performed and the analysis results documented in References 1 and 30.

The flaws identified in the Loop A upper sparger 80° downcomer thermal sleeve collar were so extensive after crack growth, that this collar is assumed to not carry load. As noted in Section 6, the piping and sparger were evaluated without the collar to establish design basis compliance and develop bounding loads for the evaluation of the 290° downcomer elbow flaw. Therefore, no flaw evaluation of the 80° collar location is provided in this section.

7.1 Flaw Evaluation Methods

These flaws are evaluated using the limit load methodology of ASME B&PV Code Section XI, Appendix C, Reference 6. This methodology assumes a plastic collapse failure mode of the flawed cross section. Plastic collapse failure occurs when the remaining uncracked ligament is assumed to reach a plastic flow stress level and behaves as a hinge at failure (Reference 7). This failure mechanism is appropriate based on the inherent fracture toughness and ductility of Type 304 austenetic stainless steels. As defined in ASME Section XI, Appendix C, the limit for plastic collapse is defined as $3S_m$ at the operating temperature. For these evaluations, the operating temperature is 550°F and the corresponding S_m is 16950.0 psi (Reference 8).

As previously stated the elbow flaws are located in the HAZ of a 100% GTAW weld. The collar flaws are adjacent to the collar to pipe weld running circumferentially around the collar (see Figures 3.1, 3.2 and 3.3). Consequently, these flaws, which are located in the HAZ of a non-flux weld root and in the collar base metal were evaluated using the base metal and the GTAW evaluation methods.

7.1.1 Flaw Characterization

Section 3 provides details of the inspection results used to characterize the flaws evaluated here. Based upon the limitations of the UT examinations, all of the flaws were conservatively evaluated as through wall. The initial circumferential lengths and the evaluated flaw lengths after 24 months and 48 months of operation are listed in Table 3.1.

The evaluation period is defined as a 48 month hot operating period. The crack growth during this period is based on the conservative IGSCC rate of $5x10^{-5}$ inches per hour as defined in Section 4. The thermal transient and expansion loads associated with the start-up, shutdown and normal operation of the vessel are insignificant. During normal operation, the internal and external pressure is equal. This eliminates any fatigue concerns associated with pipe line pressure fluctuations. Based on the low flow velocities and the rigidity (high fundamental frequency) of the core spray lines, flow induced vibrations will be negligible. Consequently, fatigue crack growth will not contribute significantly to crack growth and is not considered in the evaluated flaw length.

7.1.2 Flaw Evaluation Stress Inputs

The loads used for the flaw evaluation are taken from the piping analysis results for the core spray piping as listed in Section 6. These are the axial forces and the bending moments acting at the flaw locations for the load cases defined in Section 5 and as combined in Section 6. Reference 9 has determined that the Recirculation Line Break LOCA event produces loads which bound the Main Steam Line Break LOCA loads for this piping.

The load combinations in Section 5.2 are used in this evaluation. The worst case normal/upset, emergency/faulted, and beyond design basis faulted condition (simultaneous occurance of a seismic SSE event with Recirculation Line Break LOCA) load combinations are used for these evaluations.

Table 7.1 presents the membrane and bending stress values for the bounding design basis load combinations used to calculate the applied and allowable bending stress.

Table 7.1 Flaw Evaluation Stress Values (psi)

Flaw Location	Design Basis [1]		Beyond Design Basis	
	P_m (psi)	P_b (psi)	P_m(psi)	P_b (psi)
Loop B 110° Collar	10[1]	108	21[1]	270
	21[2]		21[2]	
Loop B 110° Elbow	0[1]	690	25[1]	901
	415[2]		439[2]	
Loop B 260° Collar	10[1]	108	21[1]	270
	21[2]		21[2]	
Loop A 290° Elbow	0[1]	698	28[1]	876
	415[2]		443[2]	

(1) The applied bending stress, P_{AB} , as defined in Equation 7-2 is based on the bounding load combination for normal/upset as well as emergency/ faulted conditions.

(2) The allowable bending stress, P_B, as defined in Equation 7-1, was calculated conservatively by using this maximum primary membrane stress from the design basis and beyond design basis load combinations.

7.1.3 Flaw Limit Load Evaluations and Results

The allowable bending stress, P_B, for the limit load evaluation was calculated using equation 7-1, Reference 6.

$$P_B = 6 \frac{S_m}{\pi} \{2 \sin(\beta) - \frac{a}{t_n} \sin(\theta)\} \qquad \text{(Eq. 7-1)}$$

$$\text{and} \quad \theta + \beta < \pi$$

$$\text{with} \quad \beta = \frac{1}{2} \{\pi - \frac{a}{t_n} \theta - \pi \frac{P_m}{3S_m}\}$$

Where θ is defined as the half angle as presented in Figure 7.1, and P_m is the membrane stress acting on the flaw. Because the flaws are assumed to be through-wall, the a/t_n ratio is equal to 1.

For these evaluations, the applied bending stress, P_{AB}, must be less than the allowable bending stress. The applied bending stress is calculated using Equation 7-2, Reference 6.

$$P_{AB} = SF (P_m + P_b) - P_m \qquad \text{(Eq. 7-2)}$$

The code safety factor (SF) is 2.77 for normal/upset and 1.39 for emergency/faulted conditions. P_m and P_b are the applied membrane and bending stress, respectively.

The flaw evaluations were performed to determine the load margin for the end of evaluated flaw size reported in Section 3. The load margin is defined as the ratio of the maximum permitted stress P_B, to the applied stress P_{AB}. This ratio

represents the margin with respect to the applied load above the ASME Section XI safety factors. In addition to the load margins, the remaining months of operation were determined by calculating maximum flaw lengths which would meet the code required safety factors. The months of operation required to reach this maximum flaw length were calculated using the bounding crack growth rate of 5×10^{-5} inch/hour. The results of these calculations are presented in Table 7.2.

Table 7.2 Flaw Evaluation Results

Flaw Locations	Load Margin Factor After 48 Months of Operation[1]		Months of Operation to Reach Critical Flaw Length	
	Design Basis	Beyond Design Basis	Design Basis	Beyond Design Basis
Loop B 110° Collar	76	63	219	217
Loop B 110° Elbow	22	16	155	150
Loop B 260° Collar	47	39	183	181
Loop A 290° Elbow	22	17	156	151

(1) This is the margin on load above and beyond the ASME Code Safety Factors of 2.77 for Normal/Upset conditions and 1.39 for Emergency/Faulted Conditions which is defined as P_B / P_{AB}.

7.2 Sensitivity Analysis

The most significant parameter influencing these flaws is the load acting on the flawed section. As previously discussed, the limit load method employed for this evaluation assumes a plastic collapse failure mechanism. Secondary or displacement controlled loads are relieved as the remaining ligament deforms plastically, thus the flaw evaluation is performed using only primary loads. The assumed plastic collapse failure mechanism is dependent on the material ductility and fracture toughness, which is appropriate for type 304 austenetic stainless steel and non-flux welds. However, materials with reduced toughness such as flux welds, may exhibit ductile tearing with net section yielding, (i.e., an elastic-plastic failure mechanism). This sensitivity analysis examines the

impact of secondary loads on the flaw structural integrity and remaining life estimates. The elbow flaws are located in the HAZ of a non-flux weld and the collar flaws are propagating in the base metal of the collar, therefore, in accordance with test results reported in References 28 and 29, and as specified in Section XI Appendix C of the ASME Code, the greater material toughness and of ductility does not warrant an examination of the elastic-plastic failure mechanism. However, this sensitivity analysis examines the impact of the secondary loads on the elbow flaw structural integrity and remaining life estimates. The following evaluations determine the load margin for the end of evaluation period flaw size from Section 3, and the remaining months of operation for the primary plus secondary loads.

7.2.1 Flaw Sensitivity Evaluations and Results

The loads used in these sensitivity evaluations are defined in the same manner as described in Section 7.1. Table 7.3 presents the membrane and bending stresses for the bounding design basis load combination as well as the "Beyond-Design-Basis" load combination.

These evaluations were performed using the simplified elastic-plastic approach defined in Section XI Appendix C of the ASME B&PV Code. This approach requires that the secondary stresses be included in a limit load formulation which uses a reduction factor Z_1, to conservatively approximate an elastic-plastic failure mechanism. The allowable bending stress, P_B, for these evaluations was calculated using equation 7-1. However the applied bending stress is modified, as stated above, to include the Z_1 factor and the secondary stresses as presented in Equation 7-3, Reference 6.

$$P_{AB} = Z_1 \ SF(P_m + P_b + P_e/SF) - P_m \qquad \text{(Eq. 7-3)}$$

Where P_e is the applied secondary load bending stress, Z_1 is defined as :

$$Z_1 = 1.15(1+ 0.013(OD-4))$$

For these flaw evaluations, the Z_1 factor is equal to 1.0 because the material toughness is sufficient to justify plastic collapse without ductile tearing.

The results of these sensitivity evaluations are presented in Table 7.4. It contains the load margins and remaining months of operation as defined in Section 7.1.3. These results demonstrate that for the limiting load cases with secondary loads and material conditions, the structural integrity of the flaws is assured.

Table 7.3 - Flaw Sensitivity Analysis Stress Values (psi)

Flaw Location	Load Type	Design Basis[1]		Beyond/Design Basis	
		P_m	P_b	P_m	P_b
Loop B 110° Elbow	Primary	25 (415)[2]	348	439 (439)[2]	438
	Secondary[3]	69	8,197	276	13,484
Loop B 110° Collar	Primary	21 (21)[2]	166	21 (21)[2]	198
	Secondary[3]	74	1,539	77	2,050
Loop B 260° Collar	Primary	21 (21)[2]	166	21 (21)[2]	198
	Secondary[3]	74	1,539	77	2,050
Loop B 290° Elbow	Primary	28 (415)[2]	307	443 (443)[2]	406
	Secondary[3]	78	9,460	292	15,319

(1) The applied bending stress, P_{AB}, as defined in Equation 7-3, includes the bounding load combinations for normal/upset as well as emergency/faulted conditions.

(2) The allowable bending stress, P_B, as defined in Equation 7-1, was calculated conservatively by using this maximum primary membrane stress from the design basis and beyond design basis load combinations.

(3) In Equation 7-3, P_e is the secondary membrane stress, P_m, conservatively added with the secondary bending stress, P_b.

Table 7.4 - Flaw Evaluation Sensitivity Analysis Results

Flaw Location	Load Margin After 48 Months of Operation[1]		Months of Operation to Reach Critical Flaw Length	
	Design Basis	Beyond Design Basis	Design Basis	Beyond Design Basis
Loop B 110° Collar	13.0	10.0	183	174
Loop B 110° Elbow	2.4	1.4	98	74
Loop B 260° Collar	8.1	6.2	146	137
Loop A 290° Elbow	2.1	1.3	93	69

(1) This is the margin on load above and beyond the ASME Code Safety Factors of 2.77 for normal/upset conditions and 1.39 for Emergency/Faulted Conditions which is defined as P_B / P_{AB} .

7.3 Flaw Evaluation Conclusions

Based on the results presented in Table 7.2, the minimum design basis load margin for the end of evaluation period flaw size is 22 and would require 155 months of operation to reach a critical flaw size. For the additional faulted condition load combination of RRLB LOCA plus an SSE, which is beyond the design basis of the Dresden Station, the minimum load margin is 16 and would require 150 months of operation to reach a critical flaw size. These results demonstrate that the flaws, projected to grow at a conservative IGSCC rate of $5x\ 10^{-5}$ in/hr for 34,560 hours, will remain structurally stable when subjected to design basis conditions. These results also demonstrate that reactor operation for more than 150 months can occur before the flaws are predicted to reach a critical length. Although the load margin and months of operation are smaller, the results from the sensitivity study (see Table 7-4) produce a similar conclusion, i.e., margins on load and operational life are significant.

Figure 7.1 - Cross Section of Flawed Pipe Model

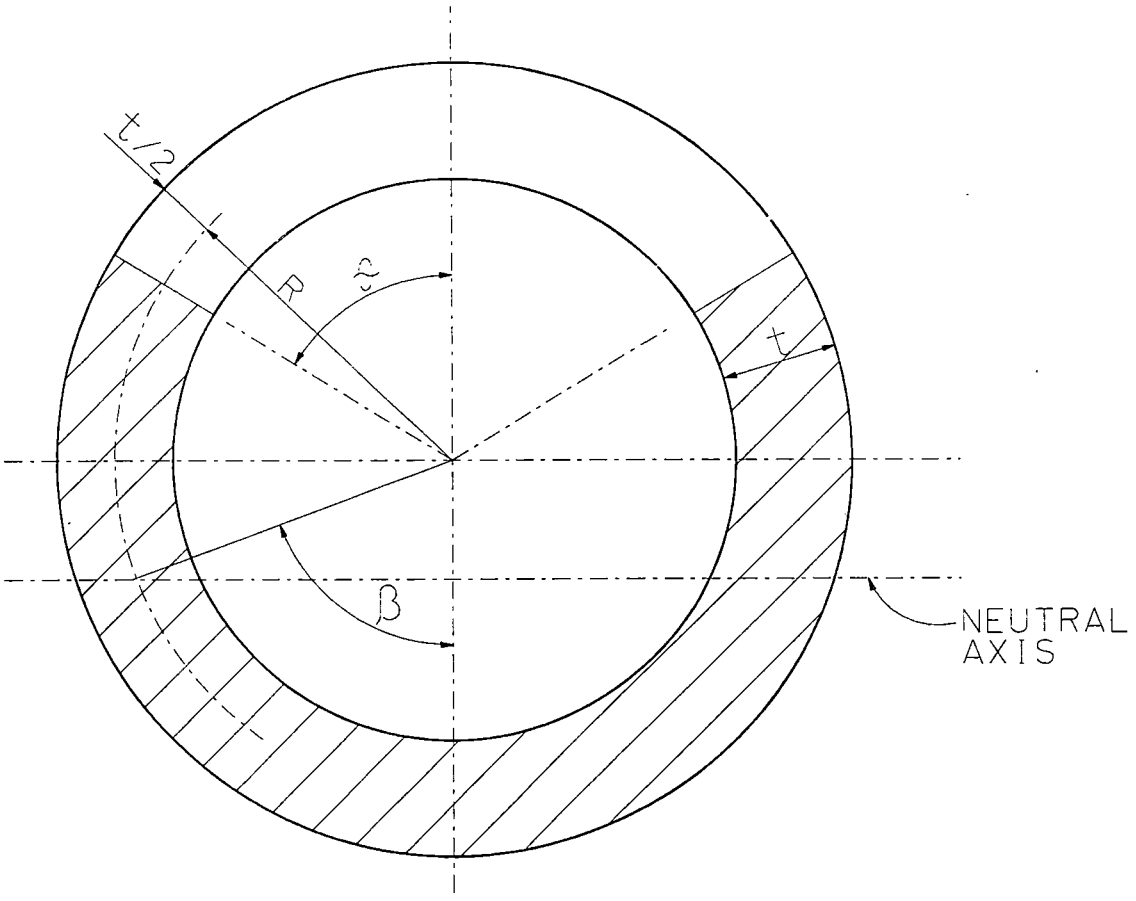

8.0 LEAKAGE FLOW EVALUATIONS

This leakage flow evaluation determines the rate that water is lost from the elbow flaws in the Loop A 290° downcomer and the Loop B 110° downcomer during core spray injection. This evaluation does not evaluate leakage from the three thermal sleeve collar flaws because these are not part of the core spray pressure boundary. The shroud penetration collar was intended to prevent leakage from inside the shroud to the annulus. The leakage from the 290° collar during normal operation was determined to be less than 0.02% of the rated core flow. This normal leakage will have minimal impact on operation. The core spray system leakage is calculated for elbow flaw lengths at the end of a 24 month and a 48 month cycle, as reported in Section 3, and at the end of life. A detailed description of the methodology and analysis techniques is provided in Section 9 of Reference 1.

8.1 Leakage Calculation Methodology

The elbow flaw leak rate is calculated using the PICEP program developed by EPRI for Leak-Before-Break applications, (Reference 14). This program uses elastic-plastic fracture mechanics to calculate the crack opening area of a through wall circumferential flaw. It calculates the leak rate based on "Henry's Homogeneous Nonequilibrium Critical Flow Model" (Reference 25). This evaluation is based on the combined membrane and bending stresses acting on the flaw from the combined loads which occur during the injection mode. The Ramberg-Osgood stress-strain parameters were obtained from Reference 26, the IPIRG Task 1.3 piping system tests database developed by Batelle, and are an average of Type 304 base metal tests at 550°F and 70°F. Because the piping temperature cools very quickly during the LOCA event and after the initiation of the core spray flow at 120°F, the line temperature is reduced to an average temperature of 195°F for this leakage calculation. Interpolation of the stress-strain data for 550°F and 70°F to 195°F, Section 23 of Reference 9, was used to establish the stress-strain input to the leakage calculations.

In this leakage flaw evaluation, the end-of-life was defined as the limiting flaw length based on the structural integrity requirements determined in Section 7 or the flaw length which produces 125 gpm leakage which ever was smaller.

8.2 Leakage Calculation Applied Loads

During the core spray injection mode, the flaw is subjected to differential pressure forces, flow induced loads and differential thermal expansion loads. The thermal load acting during the injection mode is conservatively based on the core shroud and reactor vessel being hot while the core spray piping and core shroud are cold (thermal mode 4 as described in Section 5).

The leak rates are calculated for core spray flow rates of 4500 and 5650 gpm. The minimum required flow rate corresponding to a 90 psid pressure difference between the RPV and containment (Reference 27) is 4500 gpm. The minimum required flow rate at runout (0 psid between RPV and containment, Reference 27) is 5650 gpm.

Reference 10 provides the internal core spray pipe pressure of 47 psig, at a flow rate of 4600 gpm. This pressure is scaled to the 4500 and 5650 gpm flow rates to obtain the internal pipe pressures used in the PICEP leakage calculations. The differential line pressures used for the leakage calculations are 45 psid for the 4500 gpm case and 71 psid for the 5650 gpm case.

8.3 Calculated Leakage

The PICEP leakage was calculated based on the previously described loads and material properties and is presented in Figures 8.1 through 8.4. Leak rates were calculated for 4500 gpm and 5650 gpm flow rates at the end of 24 months, 48 months and at the end-of-life condition which was limited by a maximum leakage of 125 gpm. The months of operation to reach end-of-life were based on the time needed for the measured flaws to grow to a length which produces 125 gpm leakage.

The end of life flow rates calculated here are based on the conservative thermal stresses generated from a rigid model neglecting the effects of the flexibility introduced by the flaw. The end of life flaw length will introduce significant flexibility in the system which would result in reduced bending stresses. The results of this leakage evaluation as listed in Table 8.1 are compared to the system capacity in Section 9.0 of this report.

Table 8.1 - Leak Rates at Elbow Flaws

Flaw Location	Flow Rate (gpm)		Evaluation Period	Total Leakage
Loop A 290° Elbow	4500		24 Month	11 gpm
Loop A 290° Elbow	4500		48 Month	38 gpm
Loop A 290° Elbow	4500	End-of-Life	69 Month	125 gpm
Loop A 290° Elbow	5650		24 Month	15 gpm
Loop A 290° Elbow	5650		48 Month	49 gpm
Loop B 110° Elbow	4500		24 Month	10 gpm
Loop B 110° Elbow	4500		48 Month	31 gpm
Loop B 110° Elbow	4500	End-of-Life	73 Month	125 gpm
Loop B 110° Elbow	5650		24 Month	13 gpm
Loop B 110° Elbow	5650		48 Month	41 gpm

Note: The end of life time period used here is based on the leakage limitation of 125 gpm.

Figure 8.1 - PICEP Leak Rate Loop A at 4500 GPM Flow Rate

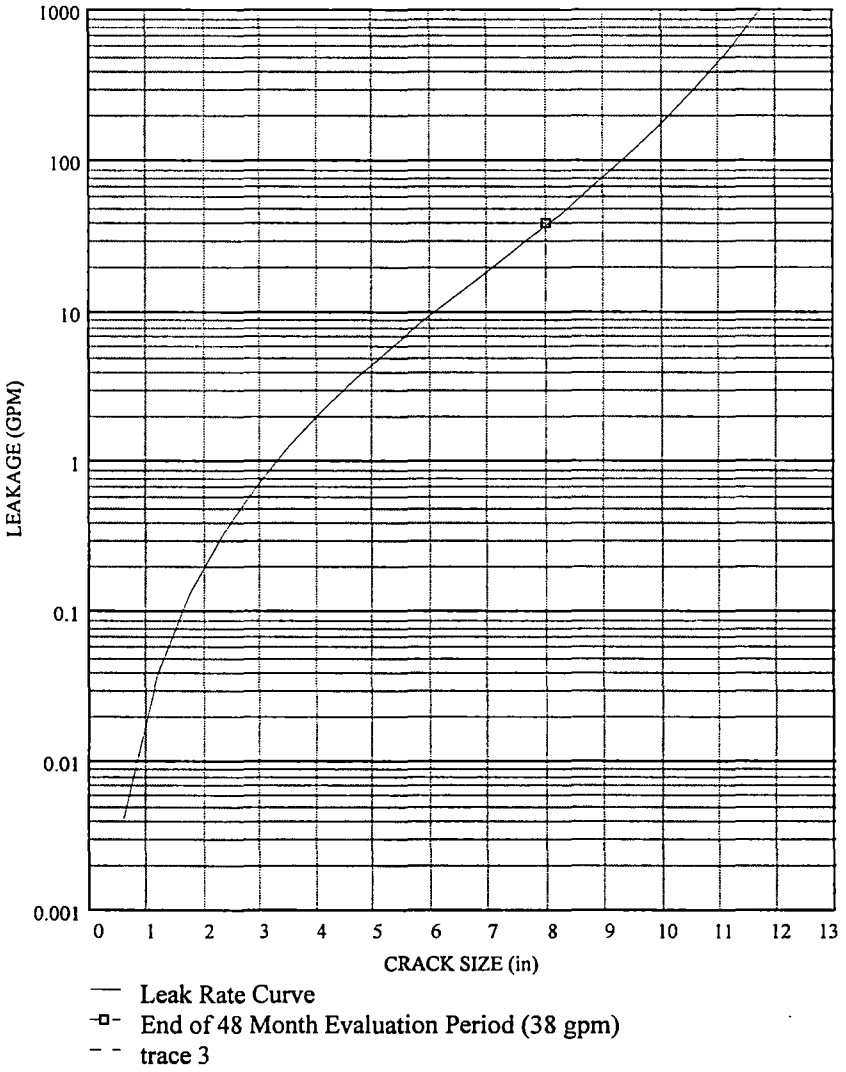

Figure 8.2 - PICEP Leak Rate Loop A at 5650 GPM Flow Rate

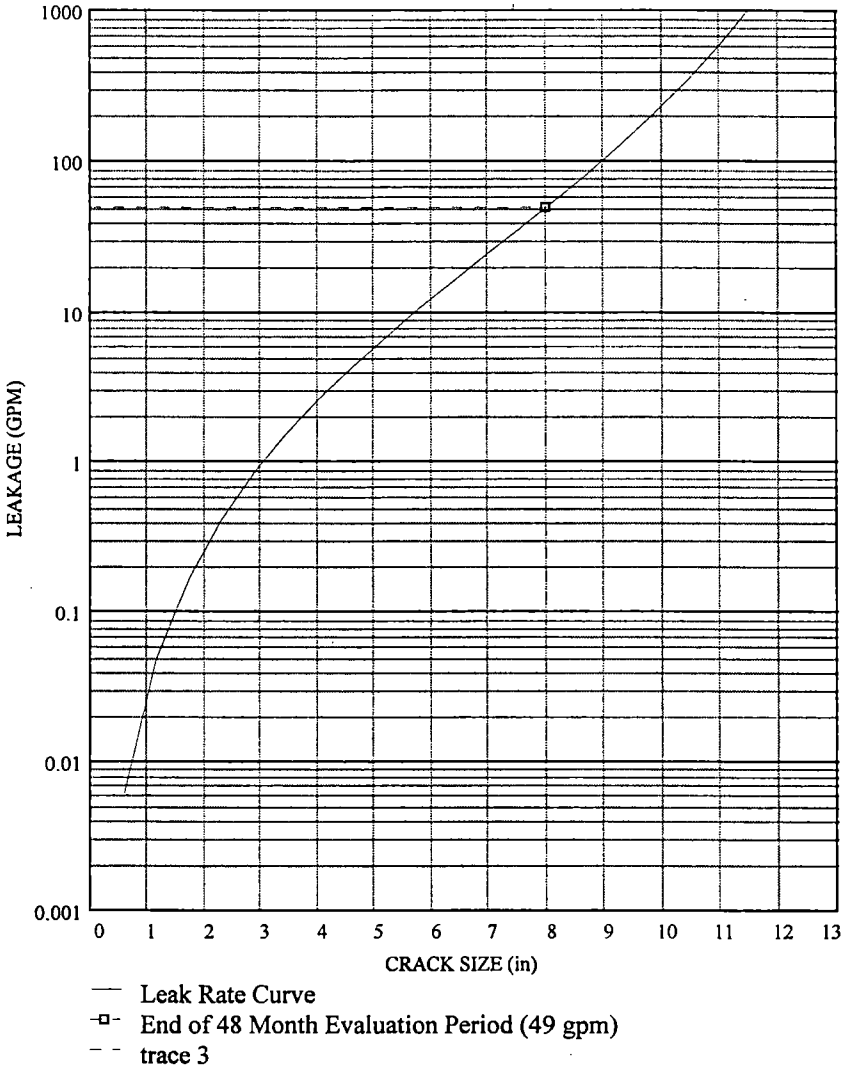

Figure 8.3 - PICEP Leak Rate Loop B at 4500 GPM Flow Rate

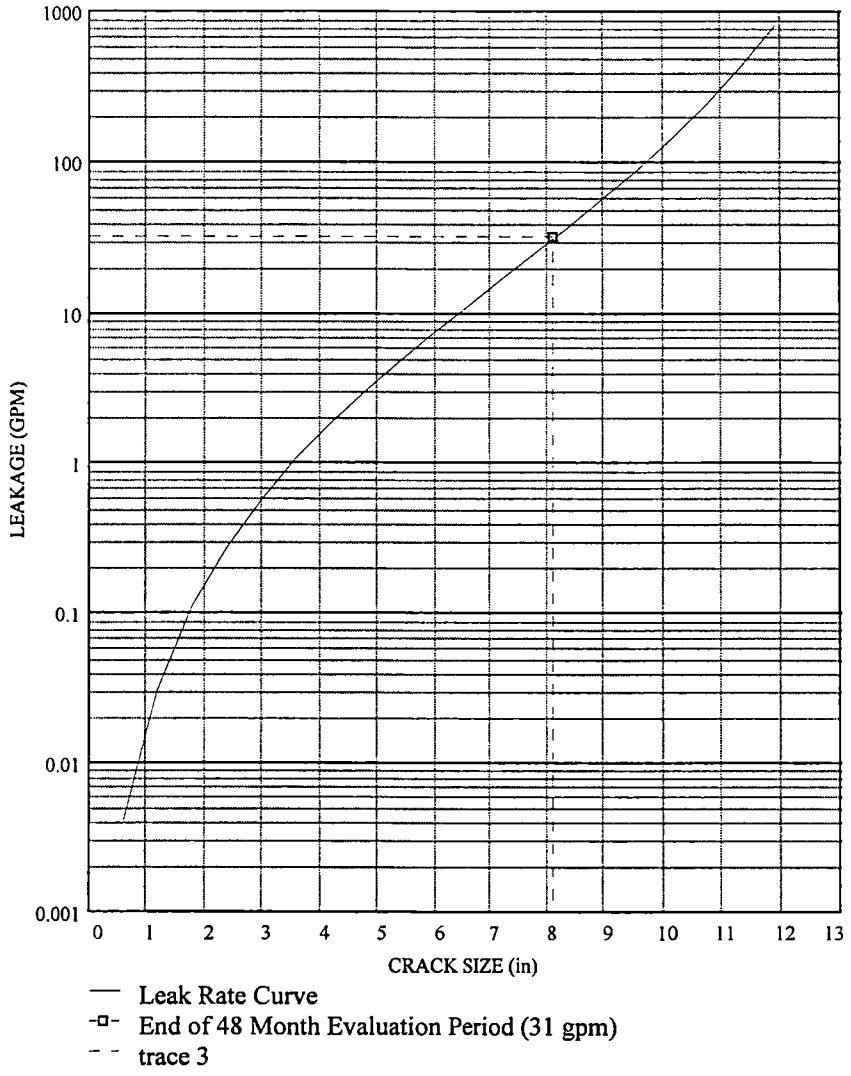

Figure 8.4 - PICEP Leak Rate Loop B at 5650 GPM Flow Rate

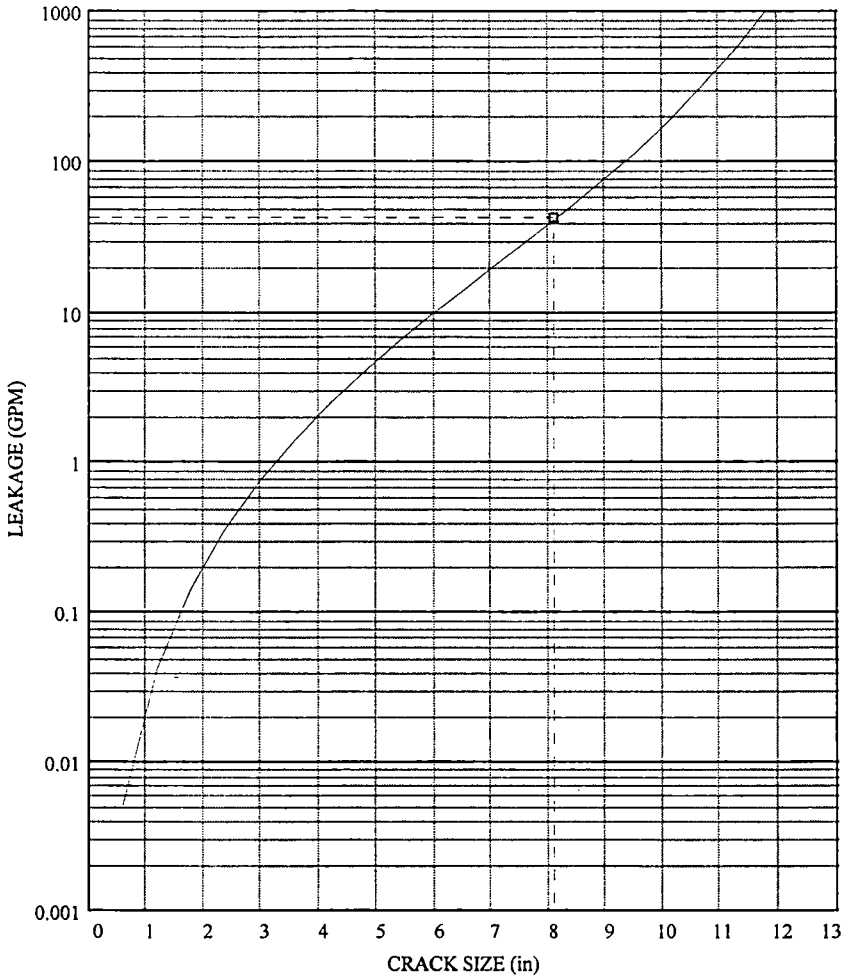

9.0 CORE SPRAY SYSTEM LOCA EVALUATION

9.1 Core Spray System Description

The core spray system along with High Pressure Coolant Injection (HPCI), Low Pressure Coolant Injection (LPCI) and Automatic Depressurization System (ADS) make up the ECCS for Dresden Unit 3. The core spray system consists of two independent redundant loops each consisting of a pump, valves, piping and independent circular sparger ring inside the core shroud just above the core. The normal water source for pump suction is the suppression pool. Each core spray pump takes suction from a common ring header that has four suction lines. A fill system is used to ensure that the core spray discharge lines remain pressurized. This fill system consists of a pump which takes suction from the suppression pool via a core spray suction line and discharges to the core spray and LPCI pump discharge lines. The power source for each core spray loop is located on an independent emergency bus. Each core spray loop is designed so that each component of the subsystem can be tested periodically.

9.2 Core Spray System Safety Function

Each core spray loop is designed to operate in conjunction with the LPCI subsystem and the ADS subsystem to provide adequate core cooling over the entire spectrum of liquid or steam pipe break sizes. For the small line break accident, the ADS and HPCI subsystems are used to depressurize the vessel to a point where the core spray and LPCI systems can be initiated in time to ensure adequate core cooling. For the large break LOCA, the depressurization assistance from HPCI or ADS is not required. For the full range of LOCA break sizes, the current licensing basis requires that core cooling be provided by both core spray loops operating together or by one core spray loop operating with two LPCI pumps (one LPCI subsystem). The core spray loops can be powered from either offsite or onsite sources.

9.3 Leakage Flow Evaluation

The bounding case for core spray is the DBA-LOCA consisting of a reactor recirculation suction line break in combination with a single failure of the LPCI

injection valve. This requires core spray to cool and reflood the core without assistance from LPCI.

The critical DBA-LOCA leakage is based on the maximum core spray flow of 4500 gpm and is 38 gpm through the Loop A elbow flaw and 31 gpm through the Loop B elbow flaw. This is based on a flaw length developed after 48 months of operation at 100% availability with crack opening based on the design basis load combinations. A leakage of 125 gpm per loop was used as the basis for determining the end of life flaw size under design basis load combinations. The flaws in the three thermal sleeve collars are not part of the core spray system pressure boundary, as they are located above the top of the core, and thus do not factor into the core spray system leakage evaluation.

During the blowdown phase of the DBA-LOCA, any core spray flow due to leakage in the annulus piping will be lost through the break. This volume of water can be directly subtracted from the core spray flow assumed in the current DBA-LOCA calculations. This would cause a decrease in liquid flow to the lower plenum during the reflood phase of the DBA-LOCA and a subsequent increase in the time required to quench the "hot node."

The current DBA-LOCA calculation, which is based on Siemens ATRIUM-9B and 9x9-2 fuel, indicates the PCT is 1920°F. Core Spray was conservatively analyzed with total reduction of 500 gpm to account for RPV penetration assembly design leakage (230 gpm), upper tee-box vent hole leakage (16 gpm), and CS piping flaws (38 + 31 = 69 gpm). Based on these numbers, only 315 gpm (230 + 16 + 69) of CS leakage exists at Dresden Unit 3, but 500 gpm of leakage was analyzed. Hence the leakage associated with the CS flaws identified in Section 8 is well within the 500 gpm of leakage analyzed for these fuel configurations.

Based on this evaluation, where the postulated leakage is bound by the conservatively analyzed leakage, there is no impact on the PCT, which is to be reported for the Siemens ATRIUM-9B and 9x9-2 fuel types.

10.0 BOUNDING FAILURE ASSESSMENT

Based on the results of the flaw evaluation in conjunction with the visual and UT inspections, the potential of developing a 360° circumferential failure in either flawed downcomer elbow is not cedible. This bounding beyond-design-basis failure assessment was performed as a means of assessing design margin. This assessment utilizes both a deterministic and probabilistic approach. The bounding failure postulates a 360° circumferential failure in any one of the four core spray downcomers that feed the spargers located inside the shroud. There are two such downcomers per core spray subsystem. Section 10.1 discusses the details of the deterministic assessment and Section 10.2 discusses the probabilistic assessment.

10.1 Deterministic Assessment

The deterministic investigation consists of an evaluation of three scenarios, each concurrent with the postulated 360° failure of any one of the four core spray downcomers. The three scenarios evaluated are:

- The DBA-LOCA; the instantaneous failure of a reactor recirculation pump suction line,
- Safe Shutdown Earthquake (SSE),
- The DBA-LOCA with the single failure of the LPCI injection valve.

The evaluation consists of postulating each scenario and demonstrating that, for each scenario adequate core cooling is provided.

10.1.1 Postulated Failure with DBA-LOCA

The DBA-LOCA is the instantaneous double end shear failure of a pipe equal in size to the largest reactor coolant system pipe. The bounding DBA-LOCA for demand on the core spray system is a reactor recirculation suction line break. Adequate core cooling can be provided even if one core spray loop is disabled due to failure of a core spray downcomer elbow in conjunction with the DBA-LOCA, since one core spray loop and one LPCI loop will remain available and can provide the required core cooling.

10.1.2 Postulated Failure with a SSE Event

The SSE is the earthquake which produces the maximum vibratory ground motion for which certain structures systems and components are designed to remain functional. The reactor vessel pressure boundary integrity would be maintained during and after a SSE event. Should core spray be required, it would only be required to re-flood the vessel and not spray on top of the core. Thus, the postulated failure of the core spray downcomer elbow would only partially divert flow from the top of the core to the lower plenum where it would effectively contribute to vessel level. Reactor coolant pressure boundary integrity allows core spray to reflood the core to assure adequate core cooling.

10.1.3 Postulated Failure with DBA-LOCA and LPCI Single Failure

This scenario combines the same DBA-LOCA discussed in Section 10.1.1 with the single failure of the LPCI injection valve. The original design basis for Dresden for a DBA-LOCA is that one core spray loop was sufficient to cool the core. Due to changes in 10CFR50.46 and Appendix K of 10CFR50 in the mid 1970's, the current design basis requires at least one core spray loop and one LPCI subsystem (two LPCI pumps) or two core spray loops to be operational to cool the core following a DBA-LOCA.

General Electric (GE) issued a Licensing Topical Report (NEDC-30936P-A, "BWR Owner's Group Technical Specification Improvement Methodology" *with Demonstration for BWR ECCS Actuation Instrumentation* Part 1, December 1988). This report was developed to identify and evaluate changes to Technical Specifications associated with Reactor Protection Systems and Emergency Core Cooling Systems (ECCS). This report states that for a BWR 3/4 of 3435 MWt reactor power, LPCI with at least 10,000 gpm capacity or Low Pressure Core Spray with at least 4600 gpm capacity and the operation of at least two Safety Relief Valves (SRVs) is sufficient to provide adequate core cooling for a BWR 3/4 plant so that the success criteria of 2200°F consistent with 10CFR50.46 is met. The results of this report are based on GE's "Realistic" LOCA model (SAFE and CHASTE computer code) which was previously reviewed and approved by the NRC for technical specification methodology.

The results of this Licensing Topical Report (Reference 11) apply to Dresden Unit 3. Dresden Unit 3 is a BWR 3 design, with a tested flow rate for one core spray loop of 4600 gpm. Core spray pump flow is periodically tested at a flow rate of 4600 gpm to ensure that the minimum rated flow of 4500 gpm is available should the need arise.

There are other parameters and conditions in the GE evaluation that are different from those existing at Dresden Unit 3. However, as discussed below the conclusions of this report are applicable to Dresden Unit 3.

- The Reactor Power of 3435 MWt is significantly higher than Dresden 2527 MWt rated thermal power. This is a conservative assumption when applied to Dresden because of a 36% higher total decay heat generation rate in the fuel.

- Dresden rated core spray flow of 4500 gpm is based on a vessel pressure of 90 psig. As the vessel continues to depressurize following the DBA-LOCA, the core spray flow will continue to increase until equilibrium is reached between the vessel and drywell or until system maximum flow is reached. The Reference 11 (NEDC-30936P-A) core spray flow of 6250 gpm appears to be a maximum flow rate. Dresden Unit 3 maximum CS flow rate has been verified as greater than 5650 GPM based on a vessel pressure of 0 psig. A surveillance test verified CS flow rates of 5800 to 5850 GPM.

- The current Dresden DBA-LOCA evaluation uses conservative estimates for other "known" leakages (i.e. through the plenum access holes, core shroud, bottom head drain line, etc.).

- This evaluation assumes that there will be no flow to the spargers through the failed core spray loop. Only one of the two downcomers would contain the postulated 360° circumferential failure, near the sleeve connection shown in Figure 2.1. Some flow will be delivered through the intact downcomer, as well as the downcomer with the postulated break if some degree of alignment is maintained.

- The Reference 11 (NEDC-30936P-A) evaluation is based on GE's fuel. For the next operating cycle, Dresden Unit 3 will utilize Siemens ATRIUM-9B and 9x9-2 fuel. These Reference 11 conclusions may or may not be

applicable to SPC 9x9-2 ATRIUM-9B fuel which have a 9x9 array. ATRIUM-9B has a large central water box and 9x9-2 has two water rods replacing fuel rods. Both fuels have different MAPLHGR limits. SPC fuel has smaller fuel pin diameters and a greater heat transfer area than the GE 8x8 fuels commonly used in 1988. These factors might result in lower PCTs compared to GE 8x8 fuel types if evaluated with an identical analysis methodology.

Thus, based on the GE Licensing Topical Report and the discussion above, for the postulated beyond design basis scenario with failure of one core spray loop due to the postulated break in the core spray downcomer elbow, core cooling could still be provided by the intact core spray loop.

10.2 Probabilistic Safety Assessment

A probabilistic evaluation was made for two scenarios. The first scenario is a reactor recirculation suction line break followed by failure of the LPCI system. The second scenario is a SSE occurring concurrently with the events in the first scenario. The probability of structural failure of a degraded core spray line was conservatively neglected. This approach is conservative because if such a structural failure had been included in the events postulated for the scenarios, then the scenario frequencies calculated below would have been multiplied by a structural failure probability estimate and the resulting probabilty too low to be considered credible.

10.2.1 Frequency Estimate for Scenario 1

The first scenario postulates a reactor recirculation suction line break followed by failure of the LPCI system. This scenario was chosen because it is within the unit's design basis, and represents the most critical case with respect to peak cladding temperature calculations. For this scenario:

Frequency of Event = Line Break Frequency x LPCI Failure Probability

The frequency of a reactor recirculation suction line break was previously estimated as 5.6×10^{-6}/year (References 15 and 16). In the Dresden PRA model for a large LOCA, LPCI failure is dominated by failure of the necessary LPCI injection path. The model for the LPCI injection path includes the loop

injection valves, loop injection check valves, loop selection logic and other supporting equipment. For a large LOCA (including a reactor recirculation suction line break), the Dresden Individual Plant Evaluation (Reference 15) gives a LPCI injection path failure probably of 2.5×10^{-3}. This value is used for the LPCI failure probability. Thus, the frequency of the postulated scenario is:

Frequency of Scenario 1 = 5.6×10^{-6}/yr x 2.51×10^{-3} = 1.4×10^{-8}/yr.

As stated above, this event probability conservatively ignores the probability of a structural failure of the core spray system.

10.2.2 Frequency Estimate for Scenario 2

The second scenario postulates a SSE concurrently with the reactor recirculation line break and failure of the LPCI system. This postulated scenario is outside the original plant design basis.

Following the approach previously used for other reactor internal evaluations (Reference 16), a concurrent SSE is postulated to occur within 24 hours of the event in Scenario 1. Thus, the frequency of this scenario is:

Frequency of Scenario 2 = (SSE Frequency)/365 x (Frequency of Scenario 1)

The frequency of a seismic event exceeding the SSE is 5×10^{-5}/yr (Reference 16). Using this value and the frequency estimate for Scenario 1 gives:

Frequency of Scenario 2 = $(5 \times 10^{-5}$/yr)/365 x 1.4×10^{-8}/yr = 2×10^{-15}/yr.

As stated above, this event probability conservatively ignores the probability of a structural failure of the core spray system.

10.2.3 Conclusions of Probabilistic Safety Assessment

Based on the low values of the calculated frequencies for the two scenarios, it can be concluded that the likelihood of the occurrence of either scenario is very small, and neither scenario is risk significant.

11.0 LOOSE PARTS EVALUATION

As part of the evaluation of the cracked core spray sparger, a scenario has been postulated where a lower elbow of a downcomer breaks off. This section of piping is assumed to fall into the vessel annulus region. An evaluation has been performed to address the safety concerns raised as a result of this loose piece.

11.1 Postulated Loose Part

The postulate loose part is a curved, stainless steel elbow. Based on the location of the observed cracks in core spray loop "B" (at the top of the elbow and in the thermal sleeve at the elbow penetration into the core shroud) the entire elbow is the most likely part to break loose. There may also be debris created as a result of rubbing and scraping of the elbow on vessel internal components.

11.2 Safety and Operational Concerns

The safety and operational concerns associated with this postulated loose part are:

- Potential for fuel bundle flow blockage and consequent fuel damage,
- Potential for fretting wear of the fuel cladding,
- Potential for interference with control rod operation,
- Potential for corrosion or chemical reaction with other reactor materials.

The elbow is postulated to break away from the core spray piping and fall into the downcomer region. This is reasonable since it is part of the piping in the annulus region outside the shroud.

11.2.1 Potential for the Fuel Bundle Flow Blockage and Consequent Fuel Damage

The elbow is located in the annulus region. Because of its size it will be unable to leave the annulus region. The jet pump throat is too small to pass the elbow

and the jet pump nozzle is far too small to pass the part into the lower plenum. Therefore, the elbow itself cannot create a fuel bundle flow blockage. Debris created by the falling part could be small enough to enter the lower plenum. Once in the lower plenum, the flow velocities are sufficiently large that the debris will be carried toward the fuel support inlet orifice. Because of its size the debris will not restrict the flow through the fuel support inlet orifice.

Depending upon the size of the debris, it may or may not pass through the lower tie plate openings. Even if it becomes trapped in the lower tie plate, the flow blockage would be quite small and distributed throughout the fuel assemblies. Therefore, no change in boiling transition effects would occur.

There is no significant concern for fuel bundle flow blockage due to the postulated generation of debris caused by the failure of a core spray downcomer elbow.

11.2.2 Potential for Fretting Wear of Fuel Cladding

If debris is created by the elbow dropping on vessel internal parts in the annulus, it could be small enough to be carried upward past the lower tie plate openings. It may become trapped at a fuel bundle spacer. This may cause the debris to rub over a small surface of a fuel rod. Prolonged operation may lead to fretting wear and leaks in the fuel rod. Any fuel cladding leaks would be detected by the off-gas system so that appropriate action can be taken to maintain the offsite radiation release within acceptable limits. Any such cladding damage would be an operational or economic concern, not a safety concern.

11.2.3 Potential for Interference with Control Rod Operation

If debris is carried past the lower tie plate it would have to travel through the fuel bundle spacers, exit the fuel channel through the upper tie plate, reverse direction, and travel downward so that it could enter the control rod guide tube. This is an extremely unlikely trajectory. The debris would have to pass through the clearance between the blade and the fuel support casting before it could enter the control rod guide tube, then pass between the velocity limiter clearance at the ID of the guide tube. Once past the velocity limiter, the debris would drop to the outer edge of the guide tube bottom if the drive was

withdrawn. Once resting there, the debris is not likely to be lifted because there is no upward flow velocity in the outer edge of the guide tube bottom. If the debris were lifted from the bottom, it would have to rise above the ridge surrounding the annulus between the index tube and the guide tube bottom, move over the annulus opening, orient itself in such a way as to enable travel through the very small gap. If it was fine enough to enter between the spud fingers, it would settle harmlessly in the inner filter. If it travelled down along the index tube OD, it would probably be captured on the outter filter. This would all occur against CRD cooling flow. This is considered highly unlikely. Even if this should happen, the debris would be very small and would not have sufficient mechanical strength to impair either the safety function (scram) or normal control rod drive operation. Consequently, there is no concern for potential interference with the CRD operation due to the postulated lost part.

11.2.4 Potential for Corrosion or Chemical Reaction with Other Reactor Materials

Since the postulated loose part is made of stainless steel, a material approved for in reactor use, there is no concern for corrosion or chemical reaction with other reactor materials.

11.3 Loose Parts Monitoring

Dresden does not have a loose-parts monitoring system. All reactor internals components and repair hardware are designed to have all pieces locked in place with mechanical devices. Hence loose parts are not anticipated. Visual inspection to identify any loose or degraded components is performed at regularly scheduled intervals.

In the remote possibility that a part of the core spray system does become loose, it would fall and rest on the jet pump support plate. The possibility of a loose part reaching the reactor fuel is even more remote. If fretting of the fuel clad did occur due to a small loose part/piece (i.e., 1/2 inch in diameter or less), the Off Gas Radiation Monitors would detect the increase in fission product release (radiation). The Dresden Technical Specifications delineate the instrumentation requirements for these monitors. Station operating procedures provide required actions when these monitors indicate elevated release rates, in order to minimize the release of fission products.

The Main Steam Line Radiation Monitors are designed to detect large changes in fission product release (gross fuel failure), and provide automatic protective functions to minimize the release of fission products. This protective function will actuate when a predetermined and preset radiation level in the main steam is reached. The Dresden Technical Specifications delineate the instrumentation requirements and setpoint for these monitors. When the setpoint is reached, an automatic action is initiated to close the main steam line isolation valves and SCRAM the reactor on MSIV closure.

11.4 Conclusion of the Loose Parts Evaluation

The safety evaluation conducted for the postulated core spray sparger elbow and debris has concluded that there is no potential for significant fuel bundle flow blockage, no safety concern due to cladding wear, no potential for interference with control rod operation and no potential for corrosion or adverse chemical reaction with other reactor materials. Thus, there are no significant safety concerns raised by the postulated break of the elbow of the core spray lower sparger inlet piping and fuel cooling throughout the core and control rod operation can be maintained.

12.0 SUMMARY AND CONCLUSIONS

NDE indications were identified at five locations on the core spray downcomers during the D3R14 in vessel inspections. This core spray line inspection was planned and implemented to meet the recommendations set forth in BWRVIP-18 (see Reference 12). The approach used to define and evaluate the flaws in the Dresden Unit 3 core spray downcomer lower elbows and shroud penetration collars was complete and thorough, and addressed all relevant parameters. The philosophy was to fully utilize all of the latest industry and plant specific information to plan and execute the inspections as well as the engineering evaluations. This is reflected in the thorough computer controlled ultrasonic testing that was performed along with the use of visual inspections to corroborate and clarify the inspection results. The stress analysis and flaw evaluations were performed using verified design inputs for all key analysis parameters. Where the analysis parameters were determined to have a significant impact on the analysis or evaluation, a conservative bounding value was selected, or a sensitivity study was performed. Provided below is a summary description of the evaluations performed along with the conclusions reached.

The details of the ultrasonic and visual examination results are defined in Section 3 of this report. The cracks were conservatively assumed to be through wall and were extended using a bounding IGSCC crack growth rate of 5.0×10^{-5} inches/hour for a 48 month operating cycle. The UT methodology developed and utilized as part of the flaw characterization was prequalified and independently verified by industry experts and is currently the best method available in the industry. The inspection methodology provided an accurate basis for performing the flaw evaluation.

The materials evaluation included a detailed assessment of the inspection records, the fabrication details, the key metallurgical analysis parameters as well as a review of relevant industry information. The review of the inspection results and pertinent industry experience indicates that the flaws are the result of IGSCC. The fabrication records were reviewed as part of the determination of the cause of the cracking as well as to identify the appropriate material properties for the flaw evaluations. The review of the material behavior and other aspects provided corroboration of the conclusion that the flaws were

IGSCC and thus a conservative crack growth rate was selected for the flaw evaluations.
The flaw evaluation was supported by a thorough and complete review of the applicable loads and load combinations for the affected piping (see Reference 1). The latest design basis information regarding RRLB, MSLB and seismic loads were incorporated into the loads definition. A detailed piping analysis was performed for the defined loading conditions. The piping modelling included such details as the rotational stiffness properties of the penetration assemblies and the gap type supports. The results of the piping analysis represent an accurate and complete definition of the critical flaw section stresses under design basis and beyond design basis load combinations. The key analysis parameters associated with the loadings, material properties and system operating conditions were reviewed and enveloped by the analyses performed.

The flaw evaluations and sensitivity study were performed using the ASME Section XI, Appendix C limit load methods. The evaluations performed include an assessment of the key analysis parameters and provides results based on the limits of these parameters. The critical elbow flaw has a load margin under design basis load combinations of 22 times the ASME code factor of safety. The critical thermal sleeve collar flaw has a load margin under design basis load combinations of 47 times the ASME code factor of safety. The sensitivity study concluded that even with consideration of all of the upper bound limits of the analysis parameters, a load margin of 2.1 times the ASME code safety factor exists for design basis load combinations for the critical elbow. These results clearly corroborate the conclusion that the core spray piping is very flaw tolerant and has sufficient margin to perform it's design basis function.

The leakage flow was calculated using a crack length corresponding to the end of 48 months of operation in conjunction with the bounding flaw section stresses. The estimated leakage of 38 gpm for Loop A and 31 gpm for Loop B for the system operating flow rate of 4500 gpm results in no increase in the peak cladding temperature (PCT), as this leakage is bound by the conservatively analyzed leakage used for the ATRIUM-9B and 9x9-2 fuel types, Reference 27.

A bounding failure assessment was performed to verify that adequate design margin exists. This assessment was performed using both a deterministic and

probabilistic approach. The deterministic approach evaluated three scenarios: 1) reactor recirculation line break, 2) SSE, and 3) reactor recirculation line break with single failure of the LPCI injection valve. In each of the scenarios, core cooling can be maintained with existing ECCS systems. The probabilistic approach postulated two scenarios: 1) reactor recirculation line break in combination with a single failure of the LPCI system and 2) reactor recirculation line break in combination with a failure of the LPCI system and concurrent SSE. The frequency of these events was calculated to be 1.4×10^{-8}/year and 2×10^{-15}/year, respectively. Thus, both scenarios can be concluded to be non-risk significant.

The potential effects of a loose part resulting from the cracked core spray sparger was evaluated. It was postulated that an elbow of the lower core spray sparger inlet piping breaks off and falls into the reactor vessel annulus region and that debris is created as a result of the rubbing and scraping of the elbow on internal vessel components. Four safety and operational concerns associated with the postulated loose part and debris were evaluated: 1) potential for fuel bundle flow blockage and consequent fuel damage, 2) potential for fretting wear of the fuel cladding, 3) potential for interference with control rod operation and 4) potential for corrosion or chemical reaction with other reactor materials. The evaluation found no significant safety or operational concerns associated with the postulated loose part or debris. The combined assessment of the system structural margin as well as core spray system functional capacity confirm the conclusion that sufficient margin exists to operate for two cycles with the identified flaws. ComEd will continue to monitor the condition of the degraded core spray welds by following the recommendations provided in BWRVIP-18 (Reference 12), during subsequent refueling outages.

13.0 REFERENCES

1. ComEd Calculation DRE97-0160, Revision 0, "Dresden Unit 3 RPV Internal Core Spray Piping and Sparger Qualification."

2. ComEd Calculation DRE96-0108, Revision 0, "Dresden Core Spray Piping and Splice Clamp."

3. Dresden RPV Thermal Cycle Diagram, GE Drawing 921D265, Rev. 1.

4. DTS 0200-02, Dresden Surveillance, In-Vessel Inspection, D3R14.

5. D3R14 Core Spray Piping Ultrasonic Examinations, GENE, April 1997, Project 1GWPY.

6. ASME B&PV Code Section XI, Appendix C, 1989.

7. Evaluations of Flaws in Austenitic Steel Piping", EPRI NP-4690-SR, July 1986.

8. ASME B&PV Code Section III, Appendix I, 1989.

9. Sargent & Lundy Calculation 9389-64-DQ.

10. GE Drawing 161F310, Revision 1, "Process Diagram - Core Spray System," Dresden Units 2 and 3.

11. NEDC-30936P-A, "BWR Owner's Group Technical Specification Improvement Methodology (with Demonstration for BWR ECCS Actuation Instrumentation) Part 1, December 1988.

12. "BWR Vessel and Internals Project-BWR Core Spray Internals Inspection and Flaw Evaluation Guidelines (BWRVIP-18)," EPRI TR-106740, July 1996.

13. NUREG-0313, Revision 2,"Technical Report on Material Selection and Processing Guidelines for BWR Coolant Pressure Boundary Piping".

14. "PICEP: Pipe Crack Evaluation Program (Revision 1)", EPRI NP-3596-SR, Revision 1, December 1987.

15. Individual Plant Evaluation Partnership (IPEP), "Dresden Nuclear Power Station Units 2 and 3, System Notebook for Low Pressure Coolant Injection System and Containment Cooling Service Water System", Revision 0, February 1993.

16. G. T. Klopp memorandum to D. H. Legler, "PRA Input to Support Dresden Shroud Cracking Evaluations," dated 5-13-94.

17. GE Drawing 104R921, Revision 3, "Assembly - Reactor Nuclear Boiler."

18. GE Drawing 104R861, Revision 10, "Assembly - Reactor Nuclear Boiler."

19. Willamette Iron & Steel Co. Drawing E861 Sheet 1, Revision H, "Dresden 2 & 3 Core Structure, Shroud."

20. Willamette Iron & Steel Co. Drawing E861 Sheet 2, Revision B, Core Structure, Shroud."

21. Willamette Iron & Steel Co. Drawing E861 Sheet 3, Revision C, "Dresden 2 & 3 Core Structure, Shroud."

22. GE Drawing 885D660 Sheet 3, Revision 4, Dresden Reactor Vessel.

23. Dresden UFSAR.

24. R H. Johnson memorandum to J. D. Williams and M. H. Richter, "Estimate of Large Recirculation Pipe Frequencies for Dresden 2 & 3 and Quad Cities 1 & 2", dated 7-11-94.

25. "The Two-Phase Critical Discharge of Initially Saturated or Subcooled Liquid," Nuclear and Engineering, 41, 1970.

26. "Pipe Fracture Database," from Douglas A. Scarth, Task Group Chairman, ASME Section XI Task Group on Pipe Flaw Evaluation, October 12, 1992.

27. "Dresden LOCA-ECCS Analysis MAPL HGR Limits for ATRIUM-9B and 9x9 Fuel," Seismic Power Corporation document EMF-97-031(P), Revision 0 dated May 1997.

28. "Instability Predictions for Circumferentially Cracked Type - 304 Stainless Under Dynamic Loading," EPRI, NP-2347, April 1982.

29. "Degraded Piping Program Phase II, Semi Annual Report, October 1984-March 1985," NUREG/CR-4082, BMI-2120, Vol. 2, July, 1985.

30. Report No. SIR-97-043, Revision 0, "Evaluation of Core Spray System Piping/Sparger Intersection at Dresden Unit 3," May 1997, Structural Integrity Associates.